

# Maximum-Area Rectangles in a Simple Polygon<sup>\*</sup>

Yujin Choi<sup>†</sup>Seungjun Lee<sup>‡</sup>Hee-Kap Ahn<sup>‡</sup>

## Abstract

We study the problem of finding maximum-area rectangles contained in a polygon in the plane. There has been a fair amount of work for this problem when the rectangles have to be axis-aligned or when the polygon is convex. We consider this problem in a simple polygon with  $n$  vertices, possibly with holes, and with no restriction on the orientation of the rectangles. We present an algorithm that computes a maximum-area rectangle in  $O(n^3 \log n)$  time using  $O(kn^2)$  space, where  $k$  is the number of reflex vertices of  $P$ . Our algorithm can report all maximum-area rectangles in the same time using  $O(n^3)$  space. We also present a simple algorithm that finds a maximum-area rectangle contained in a convex polygon with  $n$  vertices in  $O(n^3)$  time using  $O(n)$  space.

## 1 Introduction

Computing a largest figure of a certain prescribed shape contained in a container is a fundamental and important optimization problem in pattern recognition, computer vision and computational geometry. There has been a fair amount of work for finding rectangles of maximum area contained in a convex polygon  $P$  with  $n$  vertices in the plane. Amenta showed that an axis-aligned rectangle of maximum area can be found in linear time by phrasing it as a convex programming problem [3]. Assuming that the vertices are given in order along the boundary of  $P$ , stored in an array or balanced binary search tree in memory, Fischer and Höffgen gave  $O(\log^2 n)$ -time algorithm for finding an axis-aligned rectangle of maximum area contained in  $P$  [9]. The running time was improved to  $O(\log n)$  by Alt et al. [2].

Knauer et al. [13] studied a variant of the problem in which a maximum-area rectangle is not restricted to be axis-aligned while it is contained in a convex polygon. They gave randomized and deterministic approximation algorithms for the problem. Recently, Cabello et al. [6] gave an exact  $O(n^3)$ -time algorithm for finding a maximum-area rectangle with no restriction on its orientation that is contained in a convex  $n$ -gon. They also gave an algorithm for finding a maximum-perimeter rectangle and approximation algorithms.

This problem has also been studied for containers which are not necessarily convex. Some previous work on the problem focuses on finding an axis-aligned rectangle of maximum area or of maximum perimeter contained in a rectilinear polygonal container in the plane [1, 14, 15]. Daniels et al. studied the problem of finding a maximum-area axis-aligned rectangle contained in a polygon, not necessarily convex and possibly having holes [8]. They gave  $O(n \log^2 n)$ -time algorithm for the problem. Later, Boland and Urrutia improved the running time by a factor of  $O(\log n)$  for simple polygons with  $n$  vertices [5]. With no restriction on the orientation of the rectangles, Hall-Holt et al. gave a PTAS for finding a fat<sup>1</sup> rectangle of maximum area contained in a simple polygon [11].

### 1.1 Our results

We study the problem of finding a maximum-area rectangle with no restriction on its orientation that is contained in a simple polygon  $P$  with  $n$  vertices, possibly with holes, in the plane. We are not aware of any previous work on this problem, except a PTAS for finding a fat rectangle of maximum area inscribed

<sup>\*</sup>This research was supported by the MSIT(Ministry of Science and ICT), Korea, under the SW Starlab support program(IITP-2017-0-00905) supervised by the IITP(Institute of Information & communications Technology Planning & Evaluation).

<sup>†</sup>Technische Universität Berlin, Germany, Email: yj5162@postech.ac.kr

<sup>‡</sup>Pohang University of Science and Technology, Pohang, Korea, Email: {juny2400, heekap}@postech.ac.kr

<sup>1</sup>A rectangle is  $c$ -fat if its aspect ratio is at most  $c$  for some constant  $c$ .

in a simple polygon [11]. We present an algorithm that computes a maximum-area rectangle contained in a simple polygon with  $n$  vertices in  $O(n^3 \log n)$  time using  $O(kn^2)$  space, where  $k$  is the number of reflex vertices of  $P$ . Our algorithm can also find all rectangles of maximum area contained in  $P$  in the same time using  $(n^3)$  space. We also present a simple algorithm that finds a maximum-area rectangle contained in a convex polygon with  $n$  vertices in  $O(n^3)$  time using  $O(n)$  space.

To obtain the running time and space complexities, we characterize the maximum-area rectangles and classify them into six types, based on the sets of contacts on their boundaries with the polygon boundary. Then we find a maximum-area rectangle in each type so as to find a maximum-area rectangle contained in  $P$ . To facilitate the process, we construct a ray-shooting data structure for  $P$  of  $O(n)$  space which supports, for a given query point in  $P$  and a direction,  $O(\log n)$  query time. We also construct the visibility region from each vertex within  $P$ , which can be done in  $O(n^2)$  time using  $O(n^2)$  space in total. For some types, we compute locally maximal rectangles aligned to the coordinate axes while we rotate the axes. To do this, we maintain a few data structures such as double staircases of reflex vertices and priority queues for events during the rotation of the coordinate axes. They can be constructed and maintained in  $O(kn^2 \log n)$  time using  $O(kn^2)$  space. The total number of events considered by our algorithm is  $O(n^3)$ , each of which is handled in  $O(\log n)$  time.

**Theorem 1** *We can compute a largest rectangle contained in a simple polygon with  $n$  vertices, possibly with holes, in  $O(n^3 \log n)$  time using  $O(kn^2)$  space, where  $k$  is the number of reflex vertices. We can report all largest rectangles in the same time using  $O(n^3)$  space.*

**Theorem 2** *We can find a largest rectangle in a convex polygon  $P$  with  $n$  vertices in  $O(n^3)$  time using  $O(n)$  space.*

## 2 Preliminary

Let  $P$  be a simple polygon with  $n$  vertices in the plane. For ease of description, we assume that  $P$  has no hole. When  $P$  has holes, our algorithm works with a few additional data structures and procedures for testing if candidate rectangles contain a hole. We discuss this in Section 8. Without loss of generality, we assume that the vertices of  $P$  are given in order along the boundary of  $P$ . We denote by  $k$  with  $k \geq 1$  the number of reflex vertices of  $P$ . We assume the general position condition that no three vertices of  $P$  are on a line. Whenever we say a *largest rectangle*, it refers to a maximum-area rectangle contained in  $P$ .

We use the  $xy$ -Cartesian coordinate system and rotate the  $xy$ -axes around the origin while the polygon is stationary. We use  $C_\theta$  to denote the coordinate axes obtained by rotating the  $xy$ -axes of the standard  $xy$ -Cartesian coordinate system by  $\theta$  degree counterclockwise around the origin. For a point  $p$  in the plane, we use  $p_x$  and  $p_y$  to denote the  $x$ - and  $y$ -coordinates of  $p$  with respect to the coordinate axes, respectively. We say a segment or line is *horizontal* (or *vertical*) if it is parallel to the  $x$ -axis (or the  $y$ -axis). Let  $\eta(p)$ ,  $\lambda(p)$  and  $\delta(p)$  denote the ray (segment) emanating from  $p$  going horizontally leftwards, rightwards and vertically downwards in the coordinate axes, respectively, until it escapes  $P$  for the first time. We call the endpoint of a ray other than its source point the *foot* of the ray. We denote the foot of  $\eta(p)$ ,  $\lambda(p)$  and  $\delta(p)$  by  $\bar{\eta}(p)$ ,  $\bar{\lambda}(p)$  and  $\bar{\delta}(p)$ , respectively.

We use  $D_\varepsilon(p)$  to denote the disk centered at a point  $p$  with radius  $\varepsilon > 0$ . For any two points  $p$  and  $q$  in the plane, we use  $pq$  and to denote the line segment connecting  $p$  and  $q$ , and  $|pq|$  to denote the length of  $pq$ . For a segment  $s$ , we use  $D(s)$  to denote the smallest disk containing  $s$ . For a subset  $S \subseteq P$ , we define the *visibility region* of  $S$  as  $V(S) = \{x \in P \mid px \subset P \text{ for every points } p \in S\}$ . For a point  $p \in P$ , we abuse the notation such that  $V(p) = V(\{p\})$ . For a set  $X$ , we use  $\partial X$  to denote the boundary of  $X$ .

### 2.1 Existence of a maximum-area rectangle in a simple polygon

We start with showing the existence of a maximum-area rectangle contained in a simple polygon. The set  $\mathcal{G}$  of all parallelograms in the plane is a metric space under the Hausdorff distance measure  $d_H$ . The Hausdorff distance between two sets  $A$  and  $B$  of points in the plane is defined as  $d_H(A, B) = \max\{\sup_{a \in A} \inf_{b \in B} d(a, b), \sup_{b \in B} \inf_{a \in A} d(a, b)\}$ , where  $d(a, b)$  denotes the distance between  $a$  and  $b$  of the underlying metric. Since the area function  $\mu : \mathcal{G} \rightarrow \mathbb{R}^{\geq 0}$  is continuous in  $\mathcal{G}$ , the following lemma assures the existence of a largest rectangle contained in  $P$  and thus justifies the problem. Let  $\mathcal{R}$  denote the set of all rectangles contained in  $P$ . Clearly,  $\mathcal{R} \subset \mathcal{G}$ .

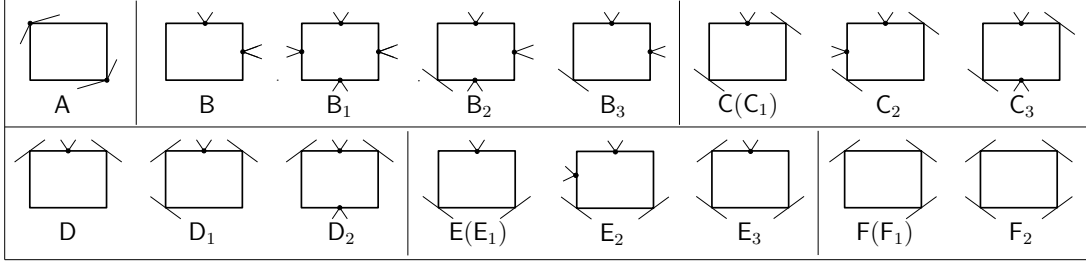


Figure 1: Classification of the determining sets of contacts of largest rectangles when rotations are allowed. Each canonical type  $X$ , except  $A$ , has a few subtypes  $X_i$  for  $i = 1, 2, 3$ .

**Lemma 3** *The set  $\mathcal{R}$  is compact.*

*Proof.* Define  $f : \mathbb{R}^6 \rightarrow \mathcal{G}$  to be a function that maps a triplet  $(p, u, v)$  of points  $p$ ,  $u$ , and  $v$  in  $\mathbb{R}^2$  to the parallelogram in  $\mathbb{R}^2$  that has  $p$ ,  $p + u$ ,  $p + v$ , and  $p + u + v$  as the four corners.

If a parallelogram  $G \in \mathcal{G}$  is not contained in  $P$ , there always exists a point  $q \in G$  and a disk  $D_\varepsilon(q)$  for some  $\varepsilon > 0$  satisfying  $D_\varepsilon(q) \cap P = \emptyset$  in the plane. Then for any parallelogram  $Q \in \mathcal{G}$  with  $d_H(G, Q) < \varepsilon$ , the intersection  $Q \cap D_\varepsilon(q)$  is not empty and  $Q$  is not contained in  $P$ . Thus,  $\mathcal{C} = \{G \in \mathcal{G} \mid G \not\subset P\}$  is open in  $\mathcal{G}$ , and therefore  $W_P = \{(p, u, v) \in \mathbb{R}^6 \mid f(p, u, v) \subset P\} = f^{-1}(\mathcal{G} \setminus \mathcal{C})$  is closed. This implies that  $T_P = \{(p, u, v) \in \mathbb{R}^6 \mid f(p, u, v) \subset P, \text{ a rectangle}\} = W_P \cap \{(p, u, v) \mid u \cdot v = 0\}$  is closed and also bounded in  $\mathbb{R}^6$ , i.e. compact. Now we can conclude that  $f(T_P) = \mathcal{R}$  is also compact by  $f$  being continuous in  $\mathbb{R}^6$ .  $\square$

## 2.2 Classification of largest rectangles

We give a classification of largest rectangles based on the sets of contacts they have on their boundaries with the polygon boundary. We say a rectangle contained in  $P$  has a *side-contact* (sc for short) if a side has a reflex vertex of  $P$  lying on it, excluding the corners. Similarly, we say a rectangle contained in  $P$  has a *corner-contact* (cc for short) if a corner lies on an edge or a vertex of  $P$ . For instance, the rectangle of case  $D_1$  in Figure 1 has a side-contact on its top side and corner-contacts on its corners, except its bottom-right corner. When two opposite corners (or two opposite sides) have corner-contacts (or side-contacts), we say the contacts are *opposite*.

Daniels et al. [8] studied this problem with restriction that rectangles must be axis-aligned. They presented a classification of determining sets of contacts, defined below, into five types for a largest axis-aligned rectangle contained in a simple polygon in the plane.

**Definition 4 (Determining set of contacts [8])** *A set  $Z$  of contacts is a determining set of contacts if the largest axis-aligned rectangle satisfying  $Z$  has finite area and the largest axis-aligned rectangle satisfying any proper subset of  $Z$  has greater or infinite area.*

In our problem, a largest rectangle  $R$  is not necessarily axis-aligned. Consider two orthogonal lines which are parallel to the sides of  $R$  and pass through the origin. Since  $R$  is aligned to the coordinate axes defined by the lines, it also has a determining set of contacts defined by Daniels et al. From this observation, we present a classification of the determining sets of contacts (DS for short) for a largest rectangle in  $P$  into six *canonical types*, from  $A$  to  $F$ , and their subtypes. The classification is given below together with figures in Figure 1.

- Type  $A$ . Exactly two opposite ccs lying on convex vertices of  $P$ .
- Type  $B$ . One sc on each side incident to a corner  $c$ . In addition,  $B_1$  has a sc on each of the other two sides, and  $B_2$  and  $B_3$  have a cc on the corner  $c'$  opposite to  $c$ .  $B_2$  has another sc on a side incident to  $c'$ .
- Type  $C$  ( $C_1$ ). Two ccs on opposite corners  $c$  and  $c'$ , and a sc on a side  $e$  incident to a corner  $c$ .  $C_2$  has another sc on the side incident to  $c'$  and adjacent to  $e$ , and  $C_3$  has another sc on a side opposite to  $e$ .

- Type D. A sc on a side  $e$  and a cc on each endpoint of  $e$ .  $D_1$  has another cc and  $D_2$  has another sc on the side opposite to  $e$ .
- Type E ( $E_1$ ). A sc on a side  $e$  and a cc on each endpoint of the side  $e'$  opposite to  $e$ .  $E_2$  has another sc on a side other than  $e$  and  $e'$ .  $E_3$  has another cc on an endpoint of  $e$ .
- Type F ( $F_1$ ). ccs on three corners.  $F_2$  has ccs on all four corners.

This classification is the same as the one by Daniels et al., except for types A, E, and F. We subdivide the last type in the classification by Daniels et al. into two types, E and F, for ease of description. A DS for type A consists of exactly two opposite corner-contacts lying on convex vertices of  $P$  while the corresponding one by Daniels et al. [8] has two opposite corners lying on the boundary (not necessarily on vertices) of  $P$ . This is because there is no restriction on the orientation of the rectangle, which is shown in Lemma 5.

**Lemma 5** *If a largest rectangle has no contact on its boundary, except two corner-contacts at opposite corners  $c$  and  $c'$ , then for every edge  $e$  of  $P$  incident to  $c$  or  $c'$ ,  $D_\varepsilon(c) \cap e$  or  $D_\varepsilon(c') \cap e$  is contained in  $D(cc')$  for some  $\varepsilon > 0$ , respectively. Thus, the corner-contacts are on convex vertices of  $P$ .*

*Proof.* Let  $R$  be a largest rectangle that has no contact on its boundary, except two corner-contacts at opposite corners  $c$  and  $c'$ . Assume to the contrary that there is no  $\varepsilon > 0$  satisfying  $D_\varepsilon(c) \cap e \subset D(cc')$  for an edge  $e$  incident to  $c$ . Then we can get another rectangle  $R'$  by rotating  $R$  around  $c'$  in a direction such that  $R'$  has no contact on its boundary, except the corner-contact at  $c'$ . Then we can get a larger rectangle by expanding  $R'$  from  $c'$  which contradicts the optimality of  $R$  under the area function  $\mu$ . We can prove the claim for edges incident to  $c'$  analogously.  $\square$

### 2.3 Maximal and breaking configurations.

Recall that  $\mathcal{R}$  denotes the set of all rectangles contained in  $P$ . Our algorithm finds a largest rectangle in  $\mathcal{R}$  of each (sub)type so as to find a largest rectangle contained in  $P$ . We call a rectangle that gives a *local maximum* of the area function  $\mu$  among rectangles in  $\mathcal{R}$  a *local maximum rectangle* (LMR for short). We say an LMR  $R$  is of type X if  $R$  has all contacts of subtype  $X_i$  for some  $i = 1, 2, \dots$ . Since a largest rectangle contained in  $P$  is a rectangle aligned to the axes that are parallel to its sides, it has contacts of at least one type defined above and is an LMR of that type. Therefore, our algorithm finds a largest rectangle among all possible LMRs of each type. If there are multiple largest rectangles, our algorithm finds them all but keeps one of them.

Consider a rectangle  $R \in \mathcal{R}$  that satisfies a DS  $Z$ . If there is no contact other than  $Z$ , there exists a continuous transformation of  $R$  such that the transformed rectangle is a rectangle contained in  $P$  and satisfying  $Z$ . Then by such a continuous transformation the area of  $R$  may change. Imagine we continue with such a transformation until the transformed rectangle  $R'$  gets another contact. In this case, we say  $R'$  is in a *breaking configuration* (BC for short) of  $Z$ . During the transformation, the area of  $R'$  may become locally maximum. If  $R'$  is locally maximum and has no contact other than  $Z$ , we say  $R'$  is in a *maximal configuration* of  $Z$ . There can be  $O(1)$  maximal configurations of  $Z$ , which can be observed from the area function of the rectangle.

**Lemma 6** *An LMR satisfying  $Z$  is in a maximal configuration or a breaking configuration.*

For a breaking configuration  $Z'$  of a DS  $Z$ , observe that  $Z' \setminus Z$  is a singleton and  $Z'$  can be a BC of some other DSs. With this fact, we can classify BCs by avoiding repetition and reducing them up to symmetry. See Figure 10 for breaking configurations.

We use  $\Gamma_\theta(Z)$  to denote the axis-aligned rectangle of largest area that satisfies a DS  $Z$  in  $C_\theta$ . We say a DS  $Z$  is *feasible* at an orientation  $\theta$  if  $\Gamma_\theta(Z)$  is a rectangle contained in  $P$ . We say an orientation  $\theta$  is *feasible* for  $Z$  if  $\Gamma_\theta(Z)$  is contained in  $P$ .

## 3 Computing a largest rectangle of type A

We show how to compute all LMRs of type A and a largest rectangle among them.

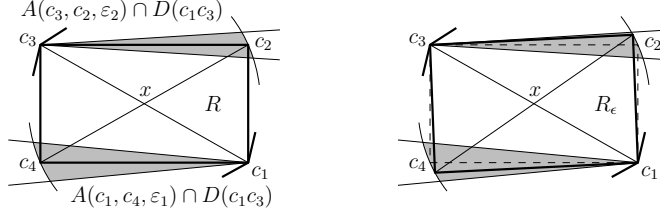


Figure 2: If an LMR  $R$  of type A is not a square, there is a larger rectangle  $R_\epsilon$ .

**Lemma 7** *Every LMR of type A is a square.*

*Proof.* Suppose there is an LMR  $R$  of type A which is not a square. Without loss of generality, assume that  $R$  has corners  $c_1, c_2, c_3$ , and  $c_4$ , from its bottom-right corner  $c_1$ , in counterclockwise order such that  $R$  has corner-contacts at  $c_1$  and  $c_3$  on convex vertices of  $P$  and  $\angle c_2 x c_1 < \frac{\pi}{2} < \angle c_3 x c_2$  for  $x = c_1 c_3 \cap c_2 c_4$ . See Figure 2. Since both  $c_2$  and  $c_4$  are contained in the interior of  $P$ , there exist  $\epsilon_1, \epsilon_2 \in (0, \frac{\pi}{4} - \frac{1}{2}\angle c_2 x c_1)$  such that  $A(c_1, c_4, \epsilon_1) \cap D(c_1 c_3) \subset P$  and  $A(c_3, c_2, \epsilon_2) \cap D(c_1 c_3) \subset P$ , where  $A(p, q, \theta) = \{x \in \mathbb{R}^2 \mid \angle x p q \in (0, \theta)\}$  for  $\theta > 0$ .

Let  $R_\epsilon$  denote the rectangle with diagonals  $c_1 c_3$  and the segment obtained by rotating  $c_2 c_4$  by  $\epsilon \in (0, 2 \min\{\epsilon_1, \epsilon_2\})$  around  $x$  in counterclockwise direction. Then  $R_\epsilon$  is contained in the union of  $R$ ,  $A(c_3, c_2, \epsilon_2) \cap D(c_1 c_3)$ , and  $A(c_1, c_4, \epsilon_1) \cap D(c_1 c_3)$ , which implies  $R_\epsilon \subset P$ . Moreover,  $\mu(R_\epsilon) > \mu(R)$  for all  $\epsilon$ , which contradicts to the assumption that  $R$  is an LMR.  $\square$

By Lemma 7, it suffices to check all possible squares in  $P$  with two opposite corners on convex vertices of  $P$ . Since  $\partial P$  is a simple closed curve, we can determine if a rectangle  $R$  is contained in  $P$  by checking if all four sides of  $R$  are contained in  $P$ .

**Lemma 8** *We can compute a largest rectangle among all LMRs of type A in  $O((n-k)n + (n-k)^2 \log n)$  time using  $O(n)$  space.*

*Proof.* We first construct a ray-shooting data structure, such as the one by Hershberger and Suri [12], for  $P$  in  $O(n)$  time using  $O(n)$  space, which supports a ray-shooting query in  $O(\log n)$  time. Then for each convex vertex  $v$  of  $P$ , we compute the list  $L$  of the vertices of  $P$  that are visible from  $v$  using  $V(v)$  in  $O(n)$  time using  $O(n)$  space.

Then for each convex vertex  $v'$  in  $L$ , we determine if the square  $S$  with diagonal  $vv'$  is contained in  $P$  by checking if each side of  $S$  is contained in  $P$  with a ray-shooting query from an endpoint along the side in  $O(\log n)$  time. The length of the ray from the query is at least  $|vv'|/\sqrt{2}$  if and only if the side is contained in  $P$ . If all four sides of  $S$  are contained in  $P$ , we compute the area of  $S$ . Among all such squares, we return one with the maximum area.  $\square$

## 4 Computing a largest rectangle of type B

We show how to compute all LMRs of type B and a largest rectangle among them. We compute for each DS a largest LMR over the maximal and breaking configurations. In doing so, we maintain a combinatorial structure for each reflex vertex which helps compute all LMRs of type B during the rotation of the coordinate axes.

### 4.1 Staircase of a point in a simple polygon

We define the staircase  $S(u)$  of a point  $u \in P$  as the set of points  $p \in P$  with  $p_x \leq u_x$  and  $p_y \leq u_y$  such that the axis-aligned rectangle with diagonal  $up$  is contained in  $P$  but no axis-aligned rectangle with diagonal  $uq$  is contained in  $P$  for any point  $q \in P$  with  $q_x < p_x$  and  $q_y < p_y$ . Thus,  $S(u)$  can be represented as a chain of segments. See Figure 3 (a).

The staircase of a point  $u \in P$  in orientation  $\theta$ , denoted by  $S_\theta(u)$ , is defined as the staircase of  $u$  in  $C_\theta$ . Every axis-aligned segment of  $S_\theta(u)$  has one endpoint at a vertex of  $P$ ,  $\bar{\eta}(u)$ , or  $\bar{\delta}(u)$ . A segment of  $S_\theta(u)$  that is not aligned to the axes is a part of an edge  $e$  of  $P$  and is called an *oblique segment*. (We say

$e$  appears to the staircase in this case.) Each vertex of  $S_\theta(u)$  which is a polygon vertex or a foot of  $\eta(u)$  or  $\delta(u)$  is called an *extremal vertex*. An extremal vertex  $v$  is called a *tip* if it is a reflex vertex of  $P$ . A vertex of  $S_\theta(u)$  contained in  $P$  is called a *hinge*. A *step* of  $S_\theta(u)$ , denoted by an ordered pair  $(a, b)$ , is the part of  $S_\theta(u)$  between two consecutive extremal vertices  $a$  and  $b$  along  $S_\theta(u)$ , where  $a_x \leq b_x$  and  $a_y \geq b_y$ . It consists of either (A) two consecutive segments  $ar$  and  $rb$  for  $r = \delta(a) \cap \eta(b)$ , or (B) three consecutive segments  $a\bar{\delta}(a)$ ,  $\bar{\delta}(a)\bar{\eta}(b)$ , and  $\bar{\eta}(b)b$  with  $\bar{\delta}(a)_x \leq \bar{\eta}(b)_x$  and  $\bar{\delta}(a)_y \geq \bar{\eta}(b)_y$ . Note that  $\bar{\delta}(a)\bar{\eta}(b)$  is the oblique segment of step  $(a, b)$  which we denote by  $\text{ob}(a, b)$ . A horizontal, vertical, or oblique segment of a step can be just a point in case of degeneracy.

We can construct  $S_\theta(u)$  for a fixed  $\theta$  in  $O(n)$  time by traversing the boundary of  $P$  in counterclockwise direction starting from  $\bar{\eta}(u)$  while maintaining the staircase of  $u$  with respect to the boundary chain traversed so far. When the next vertex  $v$  of the boundary chain satisfies  $v_x \geq t_x$  and  $v_y \leq t_y$  for the last vertex  $t$  of the current staircase, we append it to the staircase. If (part of) the edge incident to  $v$  is an oblique segment of the staircase, then we append it together with  $v$  to the staircase. If  $v_x < t_x$ , we ignore  $v$  and proceed to the vertex next to  $v$ . If  $v_x \geq t_x$  and  $v_y > t_y$ , we remove the portion of the current staircase violated by  $v$  and append  $v$  to the staircase accordingly. Observe that each vertex and each edge appear on the staircase at most once during the construction.

## 4.2 Maintaining the staircase during rotation of the coordinate system

Bae et al. [4] considered the rectilinear convex hull for a set  $Q$  of  $n$  point in the plane and presented a method of maintaining it while rotating the coordinate system in  $O(n^2)$  time. The boundary of the rectilinear convex hull consists of four maximal chains, each of which is monotone to the coordinate axes. We adopt their method and maintain the staircase of a reflex vertex  $u$  in a simple polygon.

The combinatorial structure of  $S_\theta(u)$  changes during the rotation. Figure 3 (b-f) show  $S_0(u)$ ,  $S_{\theta_1}(u)$  and  $S_{\theta_2}(u)$  for three orientations  $0, \theta_1$ , and  $\theta_2$  ( $0 < \theta_1 < \theta_2 < \pi/2$ ). Two consecutive steps,  $(a, b)$  and  $(b, c)$ , of the staircase merge into one step  $(a, c)$  when  $\bar{\delta}(a)$  meets  $b$  (Figure 3 (b)). A step  $(a, b)$  splits up into two steps  $(a, v)$  and  $(v, b)$  when  $\bar{\eta}(b)$  meets a polygon vertex  $v$  (Figure 3 (c)). A step changes its type between (A) and (B) when the hinge of a step hits a polygon edge (and then it is replaced by an oblique segment) or the oblique segment of a step degenerates to a point (and then it becomes a hinge) (Figure 3 (d)). The upper tip  $a$  (or the lower tip  $b$ ) of a step  $(a, b)$  can disappear from the staircase when  $\bar{\delta}(\bar{\eta}(u))$  meets  $a$  (or  $\bar{\eta}(\bar{\delta}(u))$  meets  $b$ ). Finally, a vertex, possibly along with an edge incident to it, can be added to or deleted from  $S_\theta(u)$  when it is met by  $\bar{\eta}(\bar{\delta}(u))$  or  $\bar{\delta}(\bar{\eta}(u))$ . We call such a change of the staircase due to the cases described above a *step event*.

One difference of the staircase  $S_\theta(u)$  to the one for a point-set by Bae et al. is that the two boundary points of  $S_\theta(u)$  are  $\bar{\eta}(u)$  and  $\bar{\delta}(u)$ . Since the polygon is not necessarily monotone with respect to the axes, the staircase may change discontinuously when  $\bar{\eta}(u)$  or  $\bar{\delta}(u)$  meets a vertex of  $P$ , which we call a *ray event*. The step of  $S_\theta(u)$  incident to  $\bar{\eta}(u)$  is replaced by a chain of  $O(n)$  steps when  $\bar{\eta}(u)$  meets a vertex of  $P$  (Figure 3 (e)). A subchain incident to  $\bar{\delta}(u)$  is replaced by a single step when  $\bar{\delta}(u)$  meets a vertex of  $P$  (Figure 3 (f)). We call the appearance or disappearance of a step caused by a ray event a *shift event* of the ray event. Note that  $O(n)$  shift events occur at a ray event. Observe that all the changes occurring in a staircase during the rotation are caused by step, ray, or shift events. We abuse  $S_\theta(u)$  to denote the combinatorial structure of the staircase if understood in context.

**Lemma 9** *Suppose a polygon edge  $e$  disappears from a step  $(a, b)$  of  $S_\theta(u)$  at  $\theta$  by a step event. Then  $e$  never appears again to the staircase during the remaining rotation until  $a_y$  becomes larger than  $u_y$  in the coordinate system.*

*Proof.* Observe that a polygon edge  $e$  of  $P$  appearing on  $S_\theta(u)$  is the oblique segment  $\text{ob}(a, b)$  of a step  $(a, b)$  which is contained in  $D(ab)$ . We claim that  $e$  disappears from the staircase at  $\theta$  when  $\text{ob}(a, b)$  degenerates to a point on  $e$  and becomes the hinge of  $(a, b)$ . Assume to the contrary that  $e$  disappears from the staircase when  $\bar{\eta}(b)$  meets a polygon vertex  $v$ . Then  $v$  becomes a new extremal vertex of the staircase by definition, and  $e$  remains on  $S_\theta(u)$  as an oblique segment  $\text{ob}(a, v)$  of step  $(a, v)$ . Similarly, it can be shown for the other types of step events that the  $e$  remains on  $S_\theta(u)$  as the oblique segment of a step in the staircase right after such an event.

Now we prove that  $e$  never appears again to the staircase as the oblique segment of a step until  $a_y$  becomes larger than  $u_y$  in the coordinate system. Let  $\theta_1$  be the orientation with  $\theta < \theta_1 < \pi/2$  that aligns

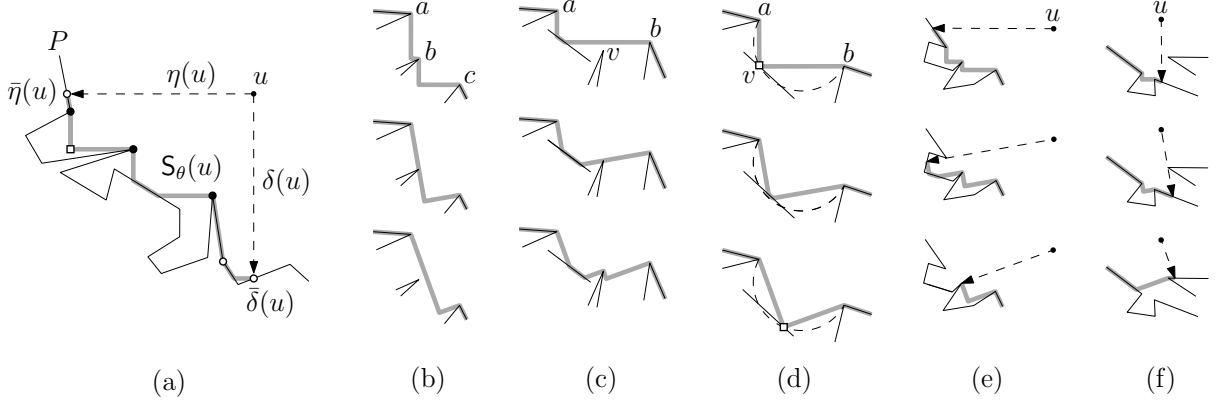


Figure 3: (a) Staircase  $S_\theta(u)$  (thick gray chain) and the tips (black disks), the extremal vertices (black disks and circles), and the hinge (square) of  $S_\theta(u)$ . (b–d) Step events, and (e–f) ray events during the rotation of the coordinate system.

$a$  and  $b$  vertically in the coordinate system rotated by  $\theta_1$ . Note that for any  $\theta' \in (\theta, \theta_1]$ , every point  $p \in e$  satisfies  $p_x < a_x$  or  $p_y < b_y$ , which implies that the axis-aligned rectangle with diagonal  $up$  contains  $a$  or  $b$  in its interior. Since  $e$  is an edge on the boundary chain from  $a$  to  $b$  counterclockwise along the boundary of  $P$ , it never appears to the staircase during the remaining rotation after  $\theta_1$  until  $a_y$  becomes larger than  $u_y$ .  $\square$

**Lemma 10** *The number of events that occur to  $S_\theta(u)$  during the rotation is  $O(n^2)$ .*

*Proof.* In the initialization at  $\theta = 0$ , there are  $O(n)$  vertices and edges in  $S_0(u)$ . A ray event occurs only if  $\bar{\eta}(u)$  or  $\bar{\delta}(u)$  meets a vertex of  $V(u)$ . Since  $\bar{\eta}(u)$  (and  $\bar{\delta}(u)$ ) meets a vertex of  $P$  at most once during the rotation, the number of ray events is  $O(n)$ , resulting with  $O(n^2)$  shift events.

Now we count the step events occurring during the rotation. Once two consecutive steps,  $(a, b)$  and  $(b, c)$ , merge into  $(a, c)$  and tip  $b$  disappears from  $S_\theta(u)$  (by the event that  $\bar{\delta}(a)$  meets  $b$ , Figure 3 (b)),  $b$  may appear again to the staircase only after  $\bar{\eta}(u)$  meets  $a$ . Similarly, a step  $(a, b)$  splits up into two steps,  $(a, v)$  and  $(v, b)$ , and a polygon vertex  $v$  appears as a tip to the staircase when  $\bar{\eta}(b)$  meets  $v$  (Figure 3 (c)). Since  $\bar{\eta}(v)$  and  $\bar{\delta}(v)$ , for any vertex  $v$ , meet another vertex of  $P$  at most once each during the rotation, a vertex appears to and disappears from the staircase  $O(n)$  times in this way. Moreover, the number of the step events occurring when  $\bar{\delta}(\bar{\eta}(u))$  or  $\bar{\eta}(\bar{\delta}(u))$  meets a polygon vertex  $v$  is  $O(n)$  for each vertex  $v$ . Thus the total number of step events occurred by  $\bar{\delta}(\bar{\eta}(u))$  and  $\bar{\eta}(\bar{\delta}(u))$  meeting polygon vertices is  $O(n^2)$ . It suffices to show that the total number of events induced by appearances or disappearances of oblique segments is  $O(n^2)$ . Lemma 9 implies that a polygon edge appears to the staircase as an oblique segment at most  $O(n)$  times during the rotation. Thus the number of events induced by oblique segments is  $O(n^2)$  in total.  $\square$

To capture these combinatorial changes and maintain the staircase during the rotation, we construct for every reflex vertex  $p$  of  $P$ , the list of segments of visibility region  $V(p)$  sorted in angular order. We compute for every pair  $(p, q)$  of reflex vertices of  $P$ , the list  $C(p, q)$  of vertices and segments of  $\partial V(\{p, q\}) \cap D(pq)$ , sorted in angular order with respect to  $p$  and  $q$ . We also compute for every pair  $(p, e)$  of a reflex vertex  $p$  and edge  $e$ , the sorted list  $L(p, e)$  of angles at which  $\bar{\delta}(\bar{\eta}(p))$  or  $\bar{\eta}(\bar{\delta}(p))$  meets a vertex of  $P$  while  $\bar{\eta}(p)$  or  $\bar{\delta}(p)$  lies on  $e$ . We store for each orientation in  $L(p, e)$  the information on the vertex corresponding to the orientation. This can be computed by finding the points that  $e$  intersects with the boundary of  $D(tp)$  for each vertex  $t$  of  $P$ . These structures together constitute the *event map*.

We also construct an *event queue* for each reflex vertex, which is a priority queue that stores events indexed by their orientations. This is to update the staircase during the rotation in a way similar to the one by Bae et al. [4] using the event map.

**Lemma 11** *The event map is of size  $O(kn^2)$  and can be constructed in  $O(kn^2 \log n)$  time.*

*Proof.* We construct event map by computing the visibility region for each vertex,  $C(p, q)$  for every pair of reflex vertices, and  $L(p, e)$  for every pair of a reflex vertex  $p$  and an edge  $e$  of  $P$ .  $V(p)$  has  $O(n)$  size

and can be computed, for each vertex  $p$ , in  $O(n)$  time.  $C(p, q)$  has  $O(n)$  size and can be computed in  $O(n)$  time as well, for each reflex vertex  $p$  and each vertex  $q$ , by cutting  $V(p) \cap V(q)$  with  $D(pq)$ . Finally, when constructing  $C(p, t)$ , we mark  $\partial D(tp) \cup e$  aligned on  $e$  for vertex  $t$  and edge  $e$  in  $O(n)$  time for each  $t$ . Then we can sort the marks to get  $L(p, e)$  in  $O(n \log n)$  time using  $O(n)$  space for each edge  $e$ . Therefore, it takes  $O(kn^2 \log n)$  time to construct the event map and its size is  $O(kn^2)$ .  $\square$

For a reflex vertex  $u$ , we maintain  $S_\theta(u)$  and the event queue  $\mathcal{Q}$  for  $u$  during the rotation using the event map. We also store the extremal vertices and edges of the staircase in a balanced binary search tree  $\mathcal{T}$  representing  $S_\theta(u)$  at the moment in order along the staircase so as to insert and delete an element in  $O(\log n)$  time. We process the events in the queue one by one in the order of priority and update the event queue.

**Lemma 12** *Once the event map is constructed,  $S_\theta(u)$  can be maintained over all events during the rotation in  $O(n^2 \log n)$  time using  $O(n)$  space. The event queue for  $u$  is maintained in the same time using  $O(n^2)$  space.*

*Proof.* There are  $O(n^2)$  events including  $O(n)$  ray events in total by Lemma 10. Therefore, the event queue can be maintained in  $O(n^2 \log n)$  time using  $O(n^2)$  space. Initially, we construct  $S_0(u)$  and  $\mathcal{T}$  in  $O(n \log n)$  time. Consider a step event that occurs on step  $(a, b)$  of  $S_\theta(u)$ :  $(a, b)$  and  $(b, c)$  merge into  $(a, c)$ ,  $(a, b)$  splits up into two steps  $(a, v)$  and  $(v, b)$ ,  $\text{ob}(a, b)$  starts to appear in  $(a, b)$ , or  $\text{ob}(a, b)$  disappears from  $(a, b)$ . We update  $S_\theta(u)$  and  $\mathcal{T}$  accordingly in  $O(\log n)$  time. Then we apply binary search on  $C(a, b)$  with query  $\delta(a)$  or  $\eta(b)$  to find the next candidate step event that may occur and change  $(a, b)$  at an orientation  $\theta' > \theta$  and to insert it into  $\mathcal{Q}$ . If the step contains  $\bar{\eta}(u)$  (or  $\bar{\delta}(u)$ ), we apply binary search on  $L(u, e)$  and  $V(v)$  with query  $\delta(\bar{\eta}(u))$  and  $\eta(v)$  (or  $\eta(\bar{\delta}(u))$  and  $\delta(v)$ ) to find next candidate step event and insert it into  $\mathcal{Q}$ . This can also be done in  $O(\log n)$  time.

Now consider a ray event caused by  $\eta(u)$  at which the tip  $q = \bar{\eta}(u)$  is removed from  $S_\theta(u)$ . We first construct  $S_\theta(q)$  and find the step on  $S_\theta(q)$  that new  $\bar{\eta}(p)$  belongs to, where  $p$  is the second tip of  $S_\theta(u)$ . From that step, we traverse  $S_\theta(q)$  up to the first extremal vertex and add the steps encountered during the traverse to  $S_\theta(u)$  (and to  $\mathcal{T}$ ). For each new step, we insert the step event candidates corresponding to the step into  $\mathcal{Q}$ , after deleting the events associated with the steps disappearing from  $\mathcal{Q}$ .

Similarly, at a ray event caused by  $\delta(u)$  when a vertex  $q = \bar{\delta}(u)$  is added to  $S_\theta(u)$  as a tip, we find the step of  $S_\theta(u)$  from  $\mathcal{T}$  which contains  $\bar{\eta}(q)$ , and delete the steps lying below  $\bar{\eta}(q)$ , together with the step event candidates associated with those deleted steps from  $\mathcal{Q}$ . We also add the new step incident to  $q$  with its step event to  $\mathcal{Q}$ . There are  $O(n)$  steps to delete. Since each deletion on  $\mathcal{T}$  can be done in  $O(\log n)$  time, a ray event and associated shift events can be handled in  $O(n \log n)$  time.  $\square$

By combining Lemmas 11 and 12, we have the following lemma.

**Lemma 13** *The staircases of all  $k$  reflex vertices of  $P$  can be constructed and maintained in  $O(kn^2 \log n)$  time using  $O(kn^2)$  space during the rotation.*

### 4.3 Data structures - double staircases, event map, and event queue

Our algorithm computes all LMRs of type B during the rotation and returns an LMR with largest area among them. To do so, it maintains for each reflex vertex  $u$  two staircases,  $S_\theta(u)$  and  $S_{\theta+\frac{\pi}{2}}(u)$  which we call the *double staircase* of  $u$ , during the rotation of the coordinate axes and computes the LMRs of type B that have  $u$  as the top sc. Let  $I$  denote the interval of orientations such that the horizontal line with respect to any  $\theta \in I$  passing through  $u$  is tangent to the boundary of  $P$  locally at  $u$ . Let  $R_\theta$  be the largest axis-aligned rectangle of type B in  $\theta \in I$  that is contained in  $P$  and has  $u$  as the top sc. Observe that every reflex vertex lying on the right side is a tip of  $S_{\theta+\frac{\pi}{2}}(u)$ . We use  $X$  to denote the contact set around the bottom-left corner  $c_\theta$  of  $R_\theta$ . Then  $X$  contains (1) a tip of  $S_\theta(u)$  touching the left side and a tip on either  $S_\theta(u)$  or  $S_{\theta+\frac{\pi}{2}}(u)$  touching the bottom side (type B<sub>1</sub>), (2) an oblique segment  $e$  on  $S_\theta(u)$  touching  $c_\theta$  and a tip on either  $S_\theta(u)$  or  $S_{\theta+\frac{\pi}{2}}(u)$  touching the bottom side (type B<sub>2</sub>), or (3) just an oblique segment  $e$  on  $S_\theta(u)$  touching  $c_\theta$  (type B<sub>3</sub>).

For a reflex vertex  $u$  of  $P$ , we construct the double staircase of  $u$ ,  $S_0(u)$  and  $S_{\frac{\pi}{2}}(u)$ . Then we maintain the event queue  $\mathcal{Q}$  containing event orientations in order: the orientations for staircase events (step and ray events) defined in previous section and the orientations at which two vertices of  $V(u)$  are aligned horizontally. The set of the orientations of the latter type is to capture the event orientations at which a tip of  $S_\theta(u)$  is aligned horizontally with a tip of  $S_{\theta+\frac{\pi}{2}}(u)$ . We call them *double staircase events*. We



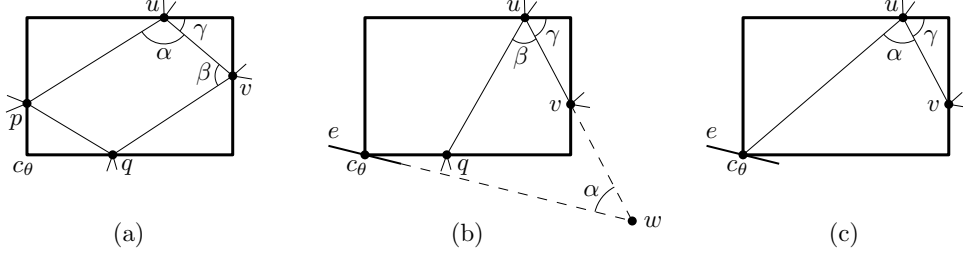


Figure 4: LMRs of (a) type  $B_1$ , (b) type  $B_2$ , and (c) type  $B_3$ .

initialize  $\mathcal{Q}$  with the latter type events. Note that it does not increase the time and space complexities of the event queue.

#### 4.4 Computing LMRs of type $B_1$

Consider a reflex vertex  $t$  of  $P$  that appears as a tip on  $S_\theta(u)$ . We use  $f(t)$  to denote the upper tip of the step on  $S_{\theta+\frac{\pi}{2}}(u)$  aligned horizontally to  $t$ . For example, in Figure 4(a,b),  $v = f(q)$  in  $S_{\theta+\frac{\pi}{2}}(u)$ . During the rotation of the coordinate axes, we consider the change of  $f(t)$  for each tip  $t$  on  $S_\theta(u)$ , as well as step, ray, and shift events on the double staircase. At each orientation,  $f(t)$  can be computed in  $O(\log n)$  time via binary search on  $S_{\theta+\frac{\pi}{2}}(u)$  with  $t_y$  since the staircase chain is monotone with respect to the  $y$ -axis. Thus we do not need to save the value  $f(t)$  for each tip  $t$ . We consider the orientation when a tip  $t$  on  $S_\theta(u)$  and  $f(t)$  on  $S_{\theta+\frac{\pi}{2}}(u)$  are aligned horizontally so that  $f(t)$  is set to the next tip on  $S_{\theta+\frac{\pi}{2}}(u)$ . At such a orientation, we detect a DS candidate of the type  $B_1$  with top, left, bottom, and right scs as  $u, p, q$ , and  $v = f(q)$ , respectively. Note that the bottom sc  $q$  might have  $q_x > u_x$ , that is,  $q$  might appear as a tip on  $S_{\theta+\frac{\pi}{2}}(u)$ . We process only the case that  $q$  is a tip on  $S_\theta(u)$ , since the other case can be handled when fixing  $p$  as an upper side contact, as described in the following, when step  $(q, v)$  disappears by a step event on  $S_{\theta+\frac{\pi}{2}}(p)$  and  $u$  is a tip on  $S_{\theta+\pi}(p)$ .

Consider an event  $E$  occurring at  $\theta$ . When a step of the double staircase that possibly contributes to a DS of type  $B_1$  changes due to  $E$ , we detect possible DSs that have been associated with it. Consider a DS  $\{u, p, q, v\}$  as in Figure 4(a). If  $E$  is a step or shift event on  $S_\theta(u)$ ,  $O(1)$  tips appear or disappear on  $S_\theta(u)$  and  $O(1)$  DSs are detected at each such event. If  $E$  is a step or shift event on  $S_{\theta+\frac{\pi}{2}}(u)$ , there are  $O(n)$  tips  $t$  on  $S_\theta(u)$  such that  $f(t)$  changes. Observe that such an event corresponds to a step event on the staircase of  $q$  in  $C_{\theta+\pi}$ . See Figure 5. Thus, we may consider only step and shift events on  $S_\theta(u)$  together with the double staircase events to detect possible DSs of type  $B_1$ .

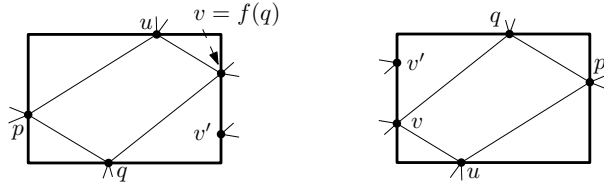


Figure 5: Step event on  $S_{\theta+\frac{\pi}{2}}(u)$  that  $f(q)$  changes from  $v$  to  $v'$  (left) which is a step event on  $S_{\theta+\pi}(q)$  (right).

We consider  $O(1)$  DSs for each event. Let  $Z = \{u, p, q, v\}$  be a DS of type  $B_1$  such that  $(p, q)$  is changed or  $q$  and  $v$  are aligned horizontally by an event  $E$  at  $\theta_E$ . Given a closed interval  $J$ , we can compute the set  $\Theta_Z$  of orientations  $\theta_Z \in J$  maximizing  $\mu(\Gamma_\theta(Z))$  locally in  $O(1)$  time because the area function  $\mu(\Gamma_\theta(Z)) = (|uv| \cos \gamma + |up| \cos(\pi - (\alpha + \gamma)))(|uv| \sin \gamma + |qv| \cos(\frac{\pi}{2} - (\beta - \gamma)))$  has  $O(1)$  extremal values in  $J$ . For angles  $\alpha, \beta, \gamma$ , see Figure 4(a).

We find the maximal interval  $J$  of orientations for  $Z = \{u, p, q, v\}$  found in an event  $E$  occurring at  $\theta_E$  such that  $\theta_E \in J$  and all elements of  $Z$  appear on the double staircase of  $u$ . This can be done by maintaining the latest orientation ( $< \theta_E$ ) at which  $(p, q)$  starts to appear as a step, the latest orientation ( $< \theta_E$ ) at which  $v$  starts to appear as a tip to the double staircase, and the orientation at which  $f(q)$  was set to  $v$ . Then  $J = [\theta_a, \theta_E]$ , where  $\theta_a$  is the latest of orientation at which all elements of  $Z$  and the step

consisting of elements of  $Z$  start to appear on the double staircase while satisfying  $f(q) = v$ . Note that the LMRs with contact  $Z$  occur at every orientation of  $\Theta_Z$  and the two endpoints (orientations) of  $J$ . Observe that the rectangle  $\Gamma_{\theta_Z}(Z)$  with  $\theta_Z \in \Theta_Z$  corresponds to a maximal configuration, and  $\Gamma_{\theta}(Z)$  with  $\theta$  being an endpoint of  $J$  corresponds to a breaking configuration. In this way, we can compute  $O(1)$  LMRs satisfying  $Z$  in  $O(1)$  time.

**Lemma 14** *Once the event map is constructed, for a fixed reflex vertex  $u$ , it takes  $O(n^2 \log n)$  time to maintain the double staircase of  $u$  and the event queue over all events during the rotation, and to compute the LMRs of type  $B_1$  having  $u$  as the top  $sc$ .*

For a reflex vertex  $u$ , we maintain an event queue  $\mathcal{Q}$ . For each event  $E$  in  $\mathcal{Q}$ , our algorithm finds  $O(1)$  DSs  $Z$  that become infeasible by  $E$ , and computes the LMRs in  $O(1)$  time. Observe that a DS  $Z$  of type  $B_1$  becomes infeasible only at shift, step, and double staircase events. Since our algorithm is applied to every reflex vertex  $u$  of  $P$ , we do not need to process the shift and step events occurring on  $S_{\theta+\frac{\pi}{2}}(u)$ . Therefore, we can detect every possible DS  $Z$  by processing the events in  $\mathcal{Q}$ . By lemmas 13 and 14,

**Lemma 15** *Our algorithm computes all LMRs of type  $B_1$  with largest area in  $O(kn^2 \log n)$  time, where  $k$  is the number of reflex vertices.*

## 4.5 Computing LMRs of type $B_2$ .

A DS  $Z = \{u, e, q, v\}$  of type  $B_2$  consists of three reflex vertices  $u, q, v$  realizing the top, bottom, right  $sc$  and an oblique segment  $e$  realizing the  $cc$  at the bottom-left corner  $c_{\theta}$  of  $\Gamma_{\theta}(Z)$ . Let  $w$  be the point where the extended line of  $e$  and the line through  $u$  and  $v$  cross. If  $w$  appears below  $c_{\theta}$ , then the area function is  $\mu(\Gamma_{\theta}(Z)) = |uq| \sin(\beta + \gamma) (\cot(\gamma - \alpha) (|uw| \sin \gamma - |uq| \sin(\beta + \gamma)) - |vw| \cos \gamma)$ . See Figure 4(b). The area of  $\Gamma_{\theta}(Z)$  with  $w$  appearing above  $u$  can be computed in a similar way. Note that there are  $O(1)$  orientations that maximize  $\mu(\Gamma_{\theta}(Z))$  locally and they can be computed in  $O(1)$  time.

Observe that  $q$  is contained in  $S_{\theta}(u)$  or  $(q, v)$  is a step on  $S_{\theta+\frac{\pi}{2}}(u)$ . In addition to the method from the Section 4.4, we also handle the case that  $(q, v)$  is a step on  $S_{\theta+\frac{\pi}{2}}(u)$  as follows. For a reflex vertex  $t$  appearing as a tip on  $S_{\theta+\frac{\pi}{2}}(u)$ , let  $g(t)$  be the edge that contains  $\bar{\eta}(t)$ . We consider every change of  $f(t)$  for each tip  $t$  on  $S_{\theta}(u)$  and the every change of  $g(t)$  for each tip  $t$  on  $S_{\theta+\frac{\pi}{2}}(u)$  during the rotation.

Consider an event  $E$  occurring at  $\theta_E$ . If  $f(q)$  changes from  $v$  to  $v'$ , we detect the DS  $\{u, e, q, v\}$ , where  $e$  is the edge containing the oblique segment of the step  $q$  belongs to, in a similar way as we process such an event of type  $B_1$ . For a step or shift event on  $S_{\theta}(u)$ , and a double staircase event, there exist only  $O(1)$  DSs becoming infeasible caused by the change of  $f(q)$ , and their LMRs are computed in  $O(1)$  time. In addition, at each event associated with disappearance of a step  $(p, q)$  on  $S_{\theta}(u)$ , we process a DS  $\{u, p, q, e\}$ , where  $e$  is the edge that contains  $\bar{\lambda}(u)$ . When  $\bar{\lambda}(u)$  no longer meets  $e$ , we process a DS  $\{u, p, q, e\}$  for each step  $(p, q)$  on  $S_{\theta}(u)$  as well. For a step or shift event on  $S_{\theta+\frac{\pi}{2}}(u)$ , there can be  $O(n)$  tips  $q$  on  $S_{\theta}(u)$  such that  $f(q)$  gets changed, but such a case overlaps with the case of step or shift event on  $S_{\theta+\pi}(q)$  with  $\bar{\lambda}(q)$  on  $e$ , which is handled for the double staircase of  $q$ . Thus we do not handle them for the double staircase of  $u$ .

So it remains to consider the case for an event  $E$  that changes  $g(q)$  for each tip  $q$  on  $S_{\theta+\frac{\pi}{2}}(u)$  at  $\theta_E$ . Observe that  $g(q)$  changes only if a double staircase event occurs associated with  $q$ . Whenever a new step  $(q, v)$  appears on  $S_{\theta+\frac{\pi}{2}}(u)$ , we do binary search for  $\bar{\eta}(q) \in e$  in  $V(q)$ . When  $g(q)$  changes or a step  $(q, v)$  disappears caused by a step or a shift event on  $S_{\theta+\frac{\pi}{2}}(u)$ , we find  $O(1)$  LMRs with DS  $Z = \{u, e, q, v\}$ , and check if they are in  $P$  by checking if the boundary of the rectangles are in  $P$ , since we do not know if  $e$  appears on  $S_{\theta}(u)$  or not. These LMRs can be computed in a similar way as we do for type  $B_1$ .

We find the maximal interval  $J$  of orientations for  $Z = \{u, e, q, v\}$  such that  $\theta_E \in J$  and all elements of  $Z$  appear on the double staircase of  $u$ . We can compute the set  $\Theta_Z$  of orientations  $\theta_Z \in J$  that maximize  $\mu(\Gamma_{\theta}(Z))$  locally in  $O(1)$  time because the area function has  $O(1)$  extremal values in  $I$ . Then for each  $\theta_Z \in \Theta_Z$ , we do binary search in  $C(q, v)$  within  $J$  for  $Z$ , to get two feasible orientations  $\theta_1, \theta_2 \in J$  closest to  $\theta_Z$  with  $\theta_1 \leq \theta_Z$  and  $\theta_2 \geq \theta_Z$  if they exist. Together with the endpoints of  $J$ , we get the LMRs with DS  $Z$ . Then we consider  $O(1)$  DSs  $Z$  of type  $B_2$  for each event and their feasible orientations that maximize the area of  $\Gamma_{\theta}(Z)$  can be computed in  $O(\log n)$  time. This way we can detect every BC including  $Z$  as well. See Figure 10. By capturing the changes of  $f(q)$  and  $g(q)$  together with the changes on the double staircase, we detect all possible DSs of type  $B_2$  and associate BCs. Suppose that an LMR appears as a  $\Gamma_{\theta}(Z)$  for  $Z = \{u, e, q, v\}$ . For example,  $e$  is on  $S_{\theta}(u)$  and  $q$  is on  $S_{\theta}(u)$  with  $f(q) = v$  or on  $S_{\theta+\frac{\pi}{2}}(u)$  with

$g(q) = e$ . As we rotate the coordinate system,  $Z$  becomes infeasible by the change of the double staircase,  $f(q)$ , or  $g(q)$ , say at event  $E$ . However, the remaining conditions are not affected by  $E$ , so that we can detect  $Z$  by our algorithm. Together with Lemma 13, we have the following lemma.

**Lemma 16** *Our algorithm computes all LMRs of  $B_2$  with the largest area in  $O(kn^2 \log n)$  time, where  $k$  is the number of reflex vertices of  $P$ .*

#### 4.6 Computing LMRs of type $B_3$ .

Consider the case when DS  $Z = \{u, e, v\}$  is feasible, where  $e$  is a polygon edge that appears as an oblique segment on  $S_\theta(u)$  and  $v$  is a tip on  $S_{\theta+\frac{\pi}{2}}(u)$  (type  $B_3$ ). See Figure 4(c). To achieve the largest area, we observe that the bottom-left corner of LMRs satisfying  $Z$  must lie at the midpoint  $c$  of the extended line segment  $pq$  of  $e$ , where  $p$  and  $q$  are the intersection points of the line containing  $e$  with  $\eta(u)$  and  $\delta(v)$ , respectively. The area function of  $\Gamma_\theta(\{u, c_\theta, v\})$ , the rectangle with top sc on  $u$ , bottom-left cc on  $c_\theta$ , and right sc on  $v$ , is convex with respect to  $c_\theta \in l$ , where  $l$  is the line containing  $e$ . If  $c$  does not lie on  $e$ ,  $c_\theta$  must lie on a point of  $e$  closest to  $c$  to maximize the rectangle area.

The area function of  $\Gamma_\theta(Z)$  for a DS  $Z$  of  $B_3$  is  $\mu(\Gamma_\theta(Z)) = |uc_\theta| \sin(\alpha + \gamma)(|uc_\theta| \cos(\pi - (\alpha + \gamma)) + |uv| \cos \gamma)$ , where  $c_\theta$  is the midpoint of  $pq$  (if the midpoint lies on  $e$ ) or the endpoint of  $e$  that is closer to the midpoint (otherwise) at  $\theta$ . Since the midpoint moves along  $l$  in one direction as  $\theta$  increases, there are  $O(1)$  intervals of orientations at which the midpoint of  $pq$  is contained in  $e$ , and thus this area function has  $O(1)$  extremal values in  $I$ .

Our algorithm for computing all LMRs of type  $B_3$  is simple. First we fix the top sc on  $u$ . For each pair of an edge  $e$  and a reflex vertex  $v$ , we compute the set  $\Theta_Z$  of orientations that maximize  $\mu(\Gamma_\theta(Z))$  locally for  $Z = \{u, e, v\}$ . Observe that  $\Theta_Z$  consists of  $O(1)$  orientations because the area function has  $O(1)$  extremal values. Then for each  $\theta_Z \in \Theta_Z$ , we find two orientations  $\theta_1, \theta_2$  closest to  $\theta_Z$  with  $\theta_1 \leq \theta_Z$  and  $\theta_2 \geq \theta_Z$  such that the top-right corner of  $\Gamma_\theta(Z)$  is contained in  $P$  by applying binary searching on  $C(u, v)$ . Finally, we check if  $\Gamma_\theta(Z)$  is contained in  $P$  for  $O(1)$  such orientations  $\theta$  by checking if the boundary of the rectangles are contained in  $P$ . This way we can compute all LMRs of  $B_3$  with top sc on  $u$ . See Figure 10. By using the event map and Lemma 13, we have the following lemma.

**Lemma 17** *Our algorithm computes all LMRs of  $B_3$  with largest area in  $O(kn^2 \log n)$  time, where  $k$  is the number of reflex vertices of  $P$ .*

### 5 Computing a largest rectangle of types C and D

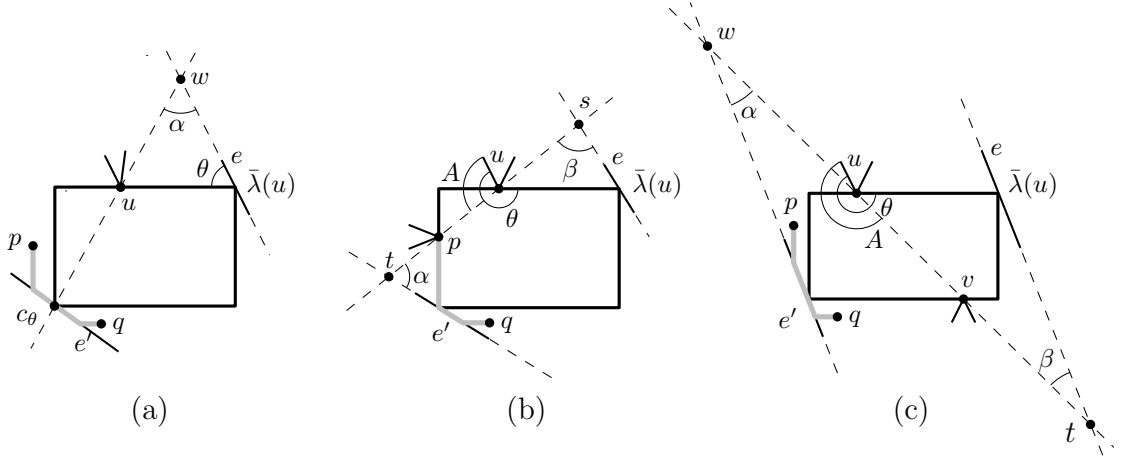
LMRs of types C and D can be computed in a way similar to the one for type B. For each reflex vertex  $u$ , we find all LMRs of types C and D that have  $u$  on its top side while maintaining the double staircase of  $u$ .

Let an edge  $e$  be an element of a DS of type C or D that is a cc on the top-right corner of an LMR. Note that  $e$  contains  $\bar{\lambda}(u)$  at some  $\theta$ .

#### 5.1 Computing LMRs of type C

As we do for type B in the Section 4, we detect the events at which a possible DS  $Z$  of type C becomes infeasible, and compute the LMRs satisfying  $Z$ . We compute LMRs of type C at (1) every step and shift event (and ray event) on  $S_\theta(u)$  such that a step on  $S_\theta(u)$  changes, (2) every ray event such that  $\bar{\lambda}(u)$  meets a vertex of  $P$ , (3) every step event of the step incident to  $\bar{\lambda}(u)$  on  $S_{\theta+\frac{\pi}{2}}(u)$ , and (4) every event such that the lower tip  $q$  of step  $(p, q)$  on  $S_\theta(u)$  and the tip  $v$  of step  $(\bar{\lambda}(u), v)$  on  $S_{\theta+\frac{\pi}{2}}(u)$  are aligned horizontally.

In case (1) such that a step  $(p, q)$  on  $S_\theta(u)$  changes, we consider three subcases: DSs  $\{u, e', e\}$  of type  $C_1$  (Figure 6(a)), DSs  $\{u, p, e', e\}$  of type  $C_2$  (Figure 6(b)), and DSs  $\{u, e, q, e'\}$  of type  $C_3$  for edge  $e'$  containing  $\text{ob}(p, q)$  (Figure 6(c)). In case (2),  $\bar{\lambda}(u)$  no longer lies on  $e$ . Thus we consider DSs  $\{u, e', e\}$  (type  $C_1$ ), DSs  $\{u, p, e', e\}$  and  $\{u, e', q, e\}$  (type  $C_2$  and  $C_3$ ), and DSs  $\{u, e', v, e\}$  (type  $C_3$ ) for each edge  $e'$  containing an oblique segment  $\text{ob}(p, q)$  on  $S_\theta(u)$  and the tip  $v$  of step  $(\bar{\lambda}(u), v)$  on  $S_{\theta+\frac{\pi}{2}}(u)$ . In case (3) such that step  $(\bar{\lambda}(u), v)$  changes, we consider three DSs  $\{u, e', e\}$ ,  $\{u, p, e', e\}$  and  $\{u, e', v, e\}$  for edge  $e'$  containing  $\text{ob}(p, q)$ , where  $(p, q)$  is the step on  $S_\theta(u)$  intersecting  $\eta(v)$ . If  $\delta(\bar{\lambda}(u))$  meets a reflex vertex  $v'$ , we consider DSs  $\{u, e', e\}$  and  $\{u, p, e', e\}$  for edge  $e'$  containing  $\text{ob}(p, q)$ , where  $(p, q)$  is the step on  $S_\theta(u)$ .



$$\begin{aligned}
\text{(a) } \text{Area}(\theta) &= |uc_\theta| \sin(\alpha + \theta)(|uw| \sin \alpha \csc \theta - |uc_\theta| \cos(\alpha + \theta)). \\
\text{(b) } \text{Area}(\theta) &= (|us| \sin \beta \csc(\theta - A - \beta) - |pu| \cos(\theta - A)) \cdot (|pu| \sin(\theta - A) - |pt| \sin \alpha \sec(\theta - A + \alpha)). \\
\text{(c) } \text{Area}(\theta) &= |uv| \sin(\theta - A)(|vw| \sin \alpha \csc(\theta - A + \alpha) + |ut| \sin \beta \csc(\theta - A + \beta) - |uv| \cos(\theta - A)).
\end{aligned}$$

Figure 6: Computing the area of some LMRs of type C. (a) Type C<sub>1</sub>, (b) type C<sub>2</sub>, and (c) type C<sub>3</sub>.

intersecting  $\eta(v')$ . For a step event of step incident to  $\bar{\lambda}(u)$ , there can be  $O(n)$  steps  $(p, q)$  on  $S_\theta(u)$  such that DSs  $\{u, e'e\}$ ,  $\{u, p, e', e\}$  and  $\{u, e', q, e\}$  for  $e'$  containing  $\text{ob}(p, q)$  become infeasible. These changes correspond to the changes caused by the step event that  $e$  disappears from  $S_{\theta+\pi}(p)$  or  $S_{\theta+\pi}(q)$ . Thus, they are handled for the double staircase of  $p$  or  $q$ . In case (4), we consider DS with  $\{u, e', v, e\}$  of type C<sub>3</sub> for step  $(\bar{\lambda}(u), v)$  on  $S_{\theta+\frac{\pi}{2}}(u)$  and edge  $e'$  containing  $\text{ob}(p, q)$ .

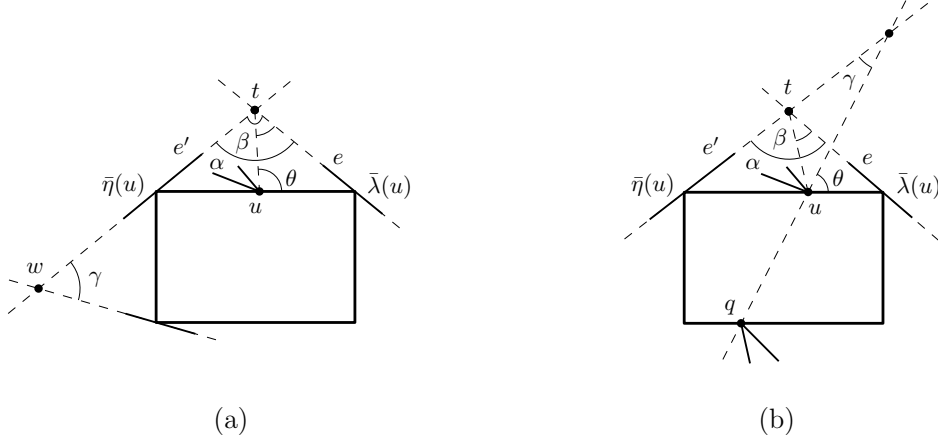
For each DS  $Z$  of type C, we have its possibly feasible interval by maintaining the orientations where each step had the last step event associated with it,  $\bar{\lambda}(u)$  met another polygon vertex, and a tip of  $S_\theta(u)$  and the lower tip  $v$  of  $(\bar{\lambda}(u), v)$  were aligned horizontally. Within such a feasible interval of a DS  $Z$ , we compute all LMRs with contact  $Z$ . It is not difficult to see that the area functions of type C<sub>2</sub> and C<sub>3</sub> depend only on  $\theta$ . And as in type B<sub>3</sub>, for a fixed  $\theta$  and  $\Gamma_\theta(Z)$  of a DS  $Z$  of type C<sub>1</sub>, the bottom-left corner  $c_\theta$  of  $\Gamma_\theta(Z)$  on  $e'$  is the midpoint of  $p = l \cap \eta(\bar{\lambda}(u))$  and  $q = l \cap \delta(\bar{\lambda}(u))$ , where  $l$  is the extended line of  $e'$ . If the midpoint does not appear on the  $S_\theta(u)$ , we simply take the point on the oblique segment contained in  $e'$  that is closest to the midpoint. This is because  $\mu(\Gamma_\theta(\{u, c_\theta, \bar{\lambda}(u)\}))$  is convex on the position of  $c_\theta$  on  $l$ . Since the number of closed intervals where the midpoint appears on  $S_\theta(u)$  is  $O(1)$ , the number of LMRs with contact  $Z$  is  $O(1)$ . As a result, for each detected DS of type C, we compute the set of  $O(1)$  orientations achieving LMRs in  $O(1)$  time.

We detect every BC of type C<sub>2</sub> with an additional top-left cc in case (1). We detect every BC of type C<sub>3</sub> with an additional bottom sc in cases (1) and (3-4) since there are two bottom scs (vertices) aligned horizontally in such a BC. The other BCs of type C with an additional top sc are detected in case (2).

## 5.2 Computing LMRs of type D

Type D is almost the same as type C, except that the base subset of DS is  $\{u, e', e\}$ , where  $e'$  and  $e$  are polygon edges containing  $\bar{\eta}(u)$  and  $\bar{\lambda}(u)$ , respectively. Moreover, instead of the bottom-left corner contacts on oblique segments of  $S_\theta(u)$  considered in type C, we simply consider corner contacts on the oblique segments of the step incident to  $\bar{\eta}(u)$  on  $S_\theta(u)$  and the step incident to  $\bar{\lambda}(u)$  on  $S_{\theta+\frac{\pi}{2}}(u)$  (Figure 7(a)) or the side contacts on the bottom side (Figure 7(b)).

Therefore, we detect DSs and BCs of types D<sub>1</sub> and D<sub>2</sub> corresponding to the events at which  $\bar{\eta}(u)$  or  $\bar{\lambda}(u)$  meets a polygon vertex, and to the step events on the step incident to  $\bar{\eta}(u)$  on  $S_\theta(u)$  or on the step events on the step incident to  $\bar{\lambda}(u)$  on  $S_{\theta+\frac{\pi}{2}}(u)$ , and to the events at which the lower tip  $q$  of step  $(\bar{\eta}(u), q)$  and the lower tip  $v$  of step  $(\bar{\lambda}(u), v)$  are aligned horizontally. There are BCs satisfying  $\{u, e', e_l, t, e\}$  of type D<sub>2</sub>, where  $t$  is a tip of  $S_{\theta+\frac{\pi}{2}}(u)$  and  $e_l$  is the edge containing  $\bar{\delta}(\bar{\eta}(u))$  (the last BC of type D<sub>2</sub> in Figure 10). We can detect such BCs of type D<sub>2</sub> that has bottom-left cc on an edge  $e_l$  in addition to the contacts  $Z = \{u, e', t, e\}$  of type D<sub>2</sub> whenever we detect DS  $Z$  in  $O(1)$  time since  $e_l$  contains an oblique



$$\begin{aligned}
 \text{(a) Area}(\theta) &= |ut| \left( \frac{\sin \beta}{\sin(\theta+\beta)} + \frac{\sin(\alpha-\beta)}{\sin(\theta-\alpha+\beta)} \right) \left( |wt| - \frac{|ut| \sin \theta}{\sin(\theta-\alpha+\beta)} \right) (\sin(\theta-\alpha+\beta) + \cos(\theta-\alpha+\beta) \tan(\gamma-\theta+\alpha-\beta)). \\
 \text{(b) Area}(\theta) &= |ut| \left( \frac{\sin \beta}{\sin(\theta+\beta)} + \frac{\sin(\alpha-\beta)}{\sin(\theta-\alpha+\beta)} \right) \cdot |uq| \sin(\theta).
 \end{aligned}$$

Figure 7: Area functions of type D. (a) Type D<sub>1</sub> and (b) type D<sub>2</sub>.

segment of the step incident to  $\bar{\eta}(u)$ . The LMRs of such a BC can be computed in  $O(1)$  time by solving basic system of linear equations.

There is another BC type of type D<sub>1</sub> that has bottom-right cc on an edge in addition to the contacts of type D<sub>1</sub>. We will handle such BCs when we handle DSs of type E<sub>3</sub> in Section 6 (the last BC of type E<sub>3</sub> in Figure 10). Thus, we exclude this BC type from the breaking configurations of type D.

**Lemma 18** *Our algorithm computes all LMRs of types C and D.*

*Proof.* By Lemma 6, an LMR satisfying a DS  $Z$  is in a maximal or breaking configuration. The DSs and BCs of type C get infeasible via one of the cases (1-4) and therefore they are detected by our algorithm. Also, the DSs and BCs of type D are handled by the step events on the step incident to  $\bar{\eta}(u)$  or  $\bar{\lambda}(u)$  of the double staircase of  $u$ .  $\square$

**Lemma 19** *We can compute a largest rectangle among all LMRs of types C and D in  $O(kn^2 \log n)$  time using  $O(kn^2)$  space, where  $k$  is the number of reflex vertices of  $P$ .*

*Proof.* The event map can be constructed in  $O(kn^2 \log n)$  time using  $O(kn^2)$  space by Lemma 11. Then for each reflex vertex, we construct its double staircase and maintain it in  $O(n^2 \log n)$  time using  $O(n)$  space by Lemma 12.

Note that for each DS or BC  $Z$  of types C and D it takes  $O(\log n)$  time to compute  $O(1)$  LMRs and check their feasibility. For each reflex vertex  $u$  as the top sc, there are  $O(n^2)$  events, and each event yields  $O(1)$  DSs or BCs in cases (1), (3) and (4). Since there are at most  $O(n)$  steps in  $S_\theta(u)$  and  $O(n)$  ray events in total, the total number of DSs handled at case (2) is  $O(n^2)$  for a reflex vertex  $u$  as the top sc. Therefore, for each reflex vertex  $u$ , we can compute LMRs of types C and D in  $O(n^2 \log n)$  time, by Lemma 18, which implies the theorem.  $\square$

## 6 Computing a largest rectangle of type E

We consider the LMRs of type E. Let  $u$  be a reflex vertex of  $P$ . We detect every DS  $Z$  of type E, containing  $\{u, e_l, e_r\}$ , where  $u$  is the top sc,  $e_l$  the bottom-left cc, and  $e_r$  the bottom-right cc. Observe that for each LMR satisfying  $Z$ ,  $e_l$  and  $e_r$  appear as oblique segments  $\text{ob}(p, q) \subset e_l$  and  $\text{ob}(t, v) \subset e_r$  of  $S_\theta(u)$  and  $S_{\theta+\frac{\pi}{2}}(u)$ , respectively, such that  $\bar{\eta}(t) \in \text{ob}(p, q)$  or  $\bar{\lambda}(q) \in \text{ob}(t, v)$ , depending on whether  $q_y \leq t_y$  or not. Using this fact, we detect the events at which  $Z$  becomes infeasible, and compute the LMRs satisfying  $Z$ .

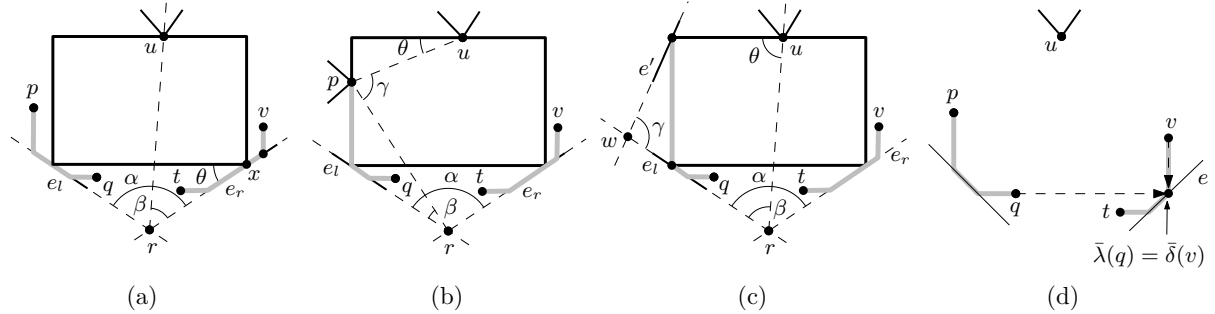
We compute LMRs of type E at (1) every step and shift event (and ray event) with a step containing an oblique segment on the double staircase, and (2) every event such that  $\bar{\lambda}(q)$  meets  $\bar{\delta}(t)$  on an edge  $e$  for a tip  $q$  of  $S_\theta(u)$  and a tip  $t$  of  $S_{\theta+\frac{\pi}{2}}(u)$  (Figure 8(d)).

In case (1), at a step or shift event with a step  $(p, q)$  on  $S_\theta(u)$  such that  $\text{ob}(p, q) \subset e_l$  is nonempty and  $\bar{\lambda}(q)$  is contained in an oblique segment  $\text{ob}(t, v) \subset e_r$  of  $S_{\theta+\frac{\pi}{2}}(u)$ , we consider DSs  $Z_1 = \{u, e_l, e_r\}$  (Figure 8(a)) and  $Z_2 = \{u, p, e_l, e_r\}$  (Figure 8(b)), together with their corresponding BCs, for edges  $e_l$  and  $e_r$  of  $P$ . A step or shift event with a step on  $S_{\theta+\frac{\pi}{2}}(u)$  can be handled in a symmetric way. If  $e_l$  appears as the oblique segment of the step incident to  $\bar{\eta}(u)$  of  $S_\theta(u)$ , we let  $Z_2 = \{u, e', e_l, e_r\}$ , where  $e'$  is the edge containing  $\bar{\eta}(u)$ . See Figure 8(c).

At an event  $E$  of case (2) occurring at  $\theta_E$ , we have a step  $(p, q)$  on  $S_\theta(u)$  and a step  $(t, v)$  on  $S_{\theta+\frac{\pi}{2}}(u)$  such that  $\bar{\lambda}(q)$  meets  $\bar{\delta}(v)$  on an edge of  $P$ . We consider the same DSs  $Z_1$  and  $Z_2$  considered in case (1). Observe that  $E$  corresponds to the step event of the double staircase of  $v$  at  $\theta_E - \frac{\pi}{2}$ . The double staircase of  $v$  has a step event at  $\theta_E - \frac{\pi}{2}$  that  $\bar{\delta}(\bar{\lambda}(v))$  meets  $q$  (equivalently,  $\bar{\lambda}(q)$  meets  $\bar{\delta}(v)$  on an edge of  $P$  at  $\theta_E$ ). See Figure 8(d).

Thus, we can capture  $E$  by maintaining the double staircase of  $v$  and insert  $E$  to the event queue of  $u$  in  $O(\log n)$  time. We compute this type of events for all reflex vertices of  $P$  by maintaining double staircases of the reflex vertices of  $P$  and insert the events to the event queues of their corresponding reflex vertices whenever such events are found. There are  $O(kn^2)$  events in total, and they can be found and inserted to the event queues in  $O(kn^2 \log n)$  time.

Whenever detecting a DS  $Z$ , we take a closed interval  $J$  of orientations at which  $Z$  is possibly feasible, and compute  $O(1)$  LMRs with contact  $Z$  within  $J$ . When  $Z$  contains  $\{u, e_l, e_r\}$  as the top sc  $u$ , bottom-left cc  $e_l$ , and bottom-right cc  $e_r$ ,  $J$  is the interval such that  $\text{ob}(p, q) \subseteq e_l$ ,  $\text{ob}(t, v) \subseteq e_r$ , and  $\bar{\lambda}(\bar{\delta}(p)) \in \text{ob}(t, v)$  or  $\bar{\lambda}(q) \in \text{ob}(t, v)$ . Note that the interval satisfying  $\bar{\lambda}(\bar{\delta}(p)) \in \text{ob}(t, v)$  or  $\bar{\lambda}(q) \in \text{ob}(t, v)$  can be computed in  $O(\log n)$  time using binary search on  $L(p, e_l)$  and  $L(v, e_r)$ . If  $Z$  contains  $p$  as the left sc or  $e'$  as the top-left cc, we consider the BCs such that  $v$  is the right sc or there is another cc on the top-right corner. Note that the BC of the second case corresponds to a BC of type D<sub>1</sub>. The orientation at which such a BC occurs can be computed in  $O(1)$  time by solving basic system of linear equations. Therefore,  $J$  can be computed in  $O(\log n)$  time.



- (a)  $\text{Area}(x, \theta) = |rx| \csc(\theta + \alpha) (|ur| \sin(\beta + \theta) - |rx| \sin \theta)$ , where  $|rx| = \frac{|ur| \sin(\beta + \theta)}{2 \sin \theta}$ .  
(b)  $\text{Area}(\theta) = |ur| \sin \alpha \cos(\gamma - \theta) \sec(\gamma - \beta) (|up| \sin \theta - |ur| \sin \beta \sec(\gamma - \beta))$ .  
(c)  $\text{Area}(\theta) = \frac{\sin \alpha \sin \gamma \tan(\theta + \beta)}{\sin(\theta + \gamma + \beta) \sin(\theta + \beta - \alpha)} (|ur| \sin \theta - |wr|) \left( \frac{|ur| \sin \theta}{\sin(\theta + \beta)} - \frac{\sin \gamma \sec(\theta + \beta)}{\sin(\gamma + \theta + \beta)} \left( \frac{|ur| \sin \theta}{\sin(\theta + \beta)} - |wr| \right) \right)$ .

Figure 8: (a-c) LMRs of type E, with reflex vertex  $u$  on the top side, and their area functions. (d) An event at  $\theta_E$  at which  $\bar{\lambda}(q)$  meets  $\bar{\delta}(v)$  on  $e$  for tips  $q$  and  $v$  and edge  $e$ .

The area functions of some cases of type E are given in Figure 8 (a-c). The area functions of the other cases of type E can be defined in a similar way. The area functions of type E have  $O(1)$  extremal values.

**Lemma 20** *Our algorithm computes all LMRs of type E.*

*Proof.* Let  $Z$  be a DS of type E such that  $Z$  is feasible at some  $\theta$ . Without loss of generality, we may assume that  $\{u, e_l, e_r\} \subset Z$ , where  $u$  is the top sc,  $e_l$  the bottom-left cc, and  $e_r$  the bottom-right cc. We also assume  $\text{ob}(p, q) \subset e_l$  for some step  $(p, q)$  of  $S_\theta(u)$ , and  $\text{ob}(t, v) \subset e_r$  for some step  $(t, v)$  of  $S_{\theta+\frac{\pi}{2}}(u)$ .

If  $Z = \{u, e_l, e_r\}$  (type  $E_1$ ),  $Z$  becomes infeasible when  $\text{ob}(p, q)$  or  $\text{ob}(t, v)$  disappears from the double staircase of  $u$  or  $\bar{\lambda}(q)$  meets  $\bar{\delta}(v)$  on  $e_r$ . We detect every event such that  $\text{ob}(p, q)$  or  $\text{ob}(t, v)$  disappears (case (1)) and every event such that  $\bar{\lambda}(q)$  meets  $\bar{\delta}(v)$  on  $e_r$  (case (2)). If  $Z$  is  $\{u, p, e_l, e_r\}$  of type  $E_2$ , it becomes infeasible by an event that we detect for DSs of type  $E_1$ . or by the step  $(p, q)$  that changes. We detect these events in cases (1) and (2) and detect the events such that step  $(p, q)$  changes in case (1). Similar to type  $E_2$ , DS  $Z = \{u, e', e_l, e_r\}$  of type  $E_3$  becomes infeasible by an event that we detect for DSs of type  $E_1$  or by a step and shift event of the step incident to  $\bar{\eta}(u)$ . Such a step and shift event is detected in case (1).

For each DS  $Z$ , we take a closed interval  $J$  of orientations where  $Z$  is possibly feasible, and therefore our algorithm computes all LMRs of type E.  $\square$

We compute  $O(1)$  LMRs for each event and check if they are contained in  $P$  in  $O(\log n)$  time. There are  $O(kn^2)$  events corresponding to case (2) which are computed in  $O(kn^2 \log n)$  time before we handle the events of type E. By Lemma 10, we have the following lemma.

**Lemma 21** *We can compute a largest rectangle among all LMRs of type E in  $O(kn^2 \log n)$  time using  $O(kn^2)$  space, where  $k$  is the number of reflex vertices of  $P$ .*

## 7 Computing a largest rectangle of type F

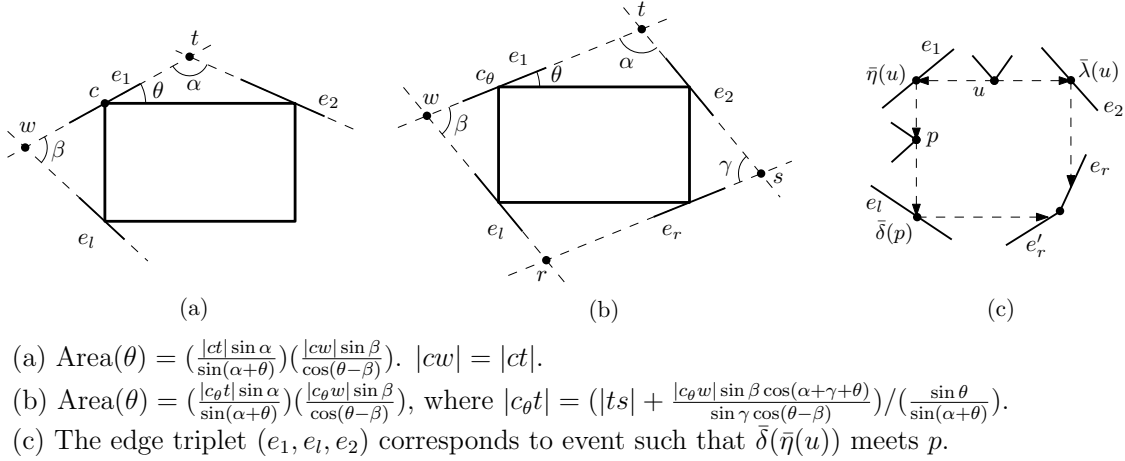


Figure 9: LMRs of type F.

To find all LMRs of type F, we compute the maximal configurations and breaking configurations of DSs of type F as follows. Consider a DS  $Z_1 = \{e_1, e_l, e_2\}$  of type  $F_1$  (Figure 9(a)) and a DS  $Z_2 = \{e_1, e_l, e_r, e_2\}$  of type  $F_2$  (Figure 9(b)). Then the LMR of a BC of type  $F_1$  is the rectangle satisfying  $Z_1 \cup \{u\}$  or  $Z_1 \cup \{e_r\}$ , or a rectangle satisfying  $Z_1$  with cc on an end vertex of an edge in  $Z_1$ , where  $u$  is a reflex vertex and  $e_r$  is an edge of  $P$ . The LMR satisfying  $Z_1 \cup \{u\}$  belongs to type  $D_1$  or  $E_3$  which is computed as an LMR of D or E, by Lemma 18 and 20. The LMR satisfying  $Z_1 \cup \{e_r\}$  belongs to type  $F_2$  and it is considered for type  $F_2$ . The LMR of a BC of type  $F_2$  is the rectangle satisfying  $Z_2 \cup \{u\}$ ,  $Z_2 \cup \{e'\}$  or the rectangle satisfying  $Z_2$  with cc on an end vertex of an edge in  $Z_2$ , where  $u$  is a reflex vertex and  $e'$  is an edge of  $P$ . The LMR satisfying  $Z_2 \cup \{u\}$  belongs to a BC of type  $E_3$  which is computed as an LMR of type E by Lemma 20. (See the last BC of type  $E_3$  in Figure 10.) Thus, we have the following lemma.

**Lemma 22** *Every LMR is of a type in  $\{A, B, C, D, E\}$ , a maximal configuration of type F, or a breaking configuration  $Z$  of type F containing a cc on an end vertex of an edge in  $Z$ .*

We say an edge pair  $(e_1, e_2)$  is *h-aligned* (and *v-aligned*) at  $\theta$  if there are points  $p_1 \in e_1$  and  $p_2 \in e_2$  such that  $p_1 p_2$  is horizontal (and vertical) and is contained in  $P$  at  $\theta$ . A pair  $(e_1, e_2)$  of edges is *h-misaligned* (and *v-misaligned*) at  $\theta$  if the pair is not h-aligned (and not v-aligned) at  $\theta$ . Note that a edge pair  $(e_1, e_2)$  changes between being h- or v-aligned and being h- or v-misaligned only when two vertices of  $P$  are

aligned horizontally or vertically during the rotation. We say a triplet  $(e_1, e_l, e_2)$  of edges *t-aligned* at  $\theta$  if there is a point  $x \in e_1$  such that  $\bar{\lambda}(x) \in e_2$  and  $\bar{\delta}(x) \in e_l$  at some  $\theta' \in \{\theta, \theta + \frac{\pi}{2}, \theta + \pi, \theta + \frac{3\pi}{2}\}$ . An edge triplet  $(e_1, e_l, e_2)$  is *t-misaligned* if it is not *t-aligned* at  $\theta$ . See Figure 9(c).

**Lemma 23** *An edge triplet  $T = (e_1, e_l, e_2)$  becomes t-misaligned only if  $(e_1, e_2)$  or  $(e_1, e_l)$  becomes h- or v-misaligned, or  $\bar{\delta}(\bar{\eta}(u))$  meets  $p$  for a vertex pair  $(u, p)$  at  $\theta$ .*

*Proof.* Without loss of generality, assume that  $T$  is *t-aligned* at  $\theta_1$  but becomes *t-misaligned* at  $\theta_2$  for any  $\theta_1 \in [\theta_2 - \varepsilon, \theta_2)$  with small  $\varepsilon > 0$ . Then there is a point  $w \in e_1$  such that  $\bar{\lambda}(w) \in e_2$  and  $\bar{\delta}(w) \in e_l$  at  $\theta_1$ . This implies that  $(e_1, e_2)$  is *h-aligned* and  $(e_1, e_l)$  is *v-aligned* at  $\theta_1$ .

Assume to the contrary that  $T$  becomes *t-misaligned* at  $\theta_2$  but  $(e_1, e_2)$  is *h-aligned*,  $(e_1, e_l)$  is *v-aligned* and no vertex pair  $(u, p)$  satisfies  $\bar{\delta}(\bar{\eta}(u))$  meeting  $p$  at  $\theta$ . Let  $X_\theta$  be the set of points  $w \in e_1$  with  $\bar{\lambda}(w) \in e_2$ , and let  $Y_\theta$  be the set of points  $w \in e_1$  with  $\bar{\delta}(w) \in e_l$  at  $\theta$ . Observe that  $X_\theta$  and  $Y_\theta$  form line segments contained in  $e_1$  and they change continuously during rotation from  $\theta_1$  to  $\theta_2$ . Since  $T$  becomes *t-misaligned* at  $\theta_2$ , there is no point  $w \in e_1$  such that  $\bar{\lambda}(w) \in e_2$  and  $\bar{\delta}(w) \in e_l$  at  $\theta_2$ , that is,  $X_{\theta_2} \cap Y_{\theta_2} = \emptyset$ . If  $X_{\theta_2} = \emptyset$ ,  $(e_1, e_2)$  is *h-misaligned*. If  $Y_{\theta_2} = \emptyset$ ,  $(e_1, e_l)$  is *v-misaligned*. The only remaining case is that  $X_{\theta_2} \neq \emptyset$  and  $Y_{\theta_2} \neq \emptyset$  but  $X_{\theta_2} \cap Y_{\theta_2} = \emptyset$ . Since  $T$  is *t-aligned* at  $\theta_1$ , that is,  $X_{\theta_1} \cap Y_{\theta_1} \neq \emptyset$ , there must be a point  $w \in e_1$  such that  $\bar{\lambda}(w)$  moves out of  $e_2$  and  $\bar{\delta}(w)$  moves out of  $e_l$  at  $\theta_2$ . This occurs when  $\bar{\lambda}(w)$  meets a vertex  $u$  and  $\bar{\delta}(w)$  meets a vertex  $p$ , that is,  $\bar{\delta}(\bar{\eta}(u))$  meets  $p$ . This gives a contradiction.  $\square$

We compute LMRs of type  $F$  at (1) every event such that two vertices are aligned horizontally or vertically, and (2) every event such that  $\bar{\delta}(\bar{\eta}(u))$  meets  $p$  for every vertex pair  $(u, p)$  at  $\theta' \in \{\theta, \theta + \frac{\pi}{2}, \theta + \pi, \theta + \frac{3\pi}{2}\}$  (Figure 9(c)). In case (1), at an event such that two vertices  $u$  and  $v$  are aligned horizontally, we find an edge pair  $(e_1, e_2)$  which becomes *h-misaligned* in  $O(\log n)$  time using ray-shooting queries with  $\eta(u)$  and  $\lambda(v)$ , assuming that  $u_x < v_x$  if such pair exists. Then we also find edges  $e_l$  and  $e_r$  such that  $e_l$  contains  $\bar{\delta}(\bar{\eta}(u))$  and  $e_r$  contains  $\bar{\delta}(\lambda(v))$ . We can find such edges in  $O(\log n)$  time using ray-shooting queries. Then we compute the set  $\Theta_{Z_i}$  of orientations that maximize  $\mu(\Gamma_\theta(Z_i))$  for each DS  $Z_1 = \{e_1, e_l, e_2\}$ ,  $Z_2 = \{e_1, e_r, e_2\}$  and  $Z_3 = \{e_1, e_l, e_r, e_2\}$  using the area functions in Figure 9 and check if  $\Gamma_\theta(Z_i)$  is contained in  $P$  for  $\theta \in \Theta_{Z_i}$ . Observe that the top-left cc of every LMR of type  $F_1$  lies at the midpoint  $c$  of  $wt$ , for the intersection  $w$  of two lines, one containing  $e_1$  and one containing  $e_l$ , and the intersection  $t$  of two lines, one containing  $e_1$  and one containing  $e_2$ . (See Figure 9 for  $wt$ .) Note that every area function in Figure 9 has  $O(1)$  extremal values. If  $c \notin e_1$ , we take the point on  $e_1$  that is closest to the midpoint. Thus, each  $\Theta_{Z_i}$  has  $O(1)$  elements and we can check for each  $\Gamma_\theta(Z_i)$  if it is contained in  $P$  in  $O(\log n)$  using ray-shooting queries. We also compute the BCs satisfying  $Z_i$  with cc on an end vertex of an edge in  $Z_i$ , and check their feasibility. There are  $O(1)$  such BCs which can be computed in  $O(1)$  time. We can compute in  $O(1)$  time  $\mu(\Gamma_\theta(Z))$  for each BC  $Z$ . An event at which two vertices  $u$  and  $v$  are aligned vertically can be handled in a symmetric way.

In case (2), when  $\bar{\delta}(\bar{\eta}(u))$  meets  $p$ , we find an edge triplet  $(e_1, e_l, e_2)$  which becomes *t-misaligned* in  $O(\log n)$  time using ray-shooting queries with  $\eta(u)$ ,  $\lambda(u)$  and  $\delta(p)$ . We also find edges  $e_r$  and  $e'_r$  such that  $\bar{\delta}(\lambda(u)) \in e_r$  and  $\bar{\lambda}(p) \in e'_r$  in  $O(\log n)$  time using ray-shooting queries. Similar to case (1), we compute  $\Theta_{Z_i}$  for each DS  $Z_1 = \{e_1, e_l, e_2\}$ ,  $Z_2 = \{e_1, e_l, e_r, e_2\}$  and  $Z_3 = \{e_1, e_l, e'_r, e_2\}$  and check if  $\Gamma_\theta(Z_i) \subseteq P$  for  $\theta \in \Theta_{Z_i}$ . Then we compute the BCs satisfying  $Z_i$  with cc on an end vertex of an edge in  $Z_i$  and check their feasibility.

**Lemma 24** *Our algorithm computes all maximal configurations of type  $F$  and all breaking configurations of type  $F$  which contain a cc on a vertex of  $P$ .*

*Proof.* Let  $Z_1 = \{e_1, e_l, e_2\}$  and  $Z_2 = \{e_1, e_l, e_r, e_2\}$  be a DS of type  $F_1$  and  $F_2$ , respectively, and assume they are feasible at some  $\theta$ . There are three events corresponding to  $Z_1$ ,  $(e_1, e_2)$  becomes *h-misaligned* at  $\theta_1$ ,  $(e_1, e_l)$  becomes *v-misaligned* at  $\theta_2$  and  $(e_1, e_l, e_2)$  becomes *t-misaligned* at  $\theta_3$ . Let  $\theta'$  be the smallest one among  $\theta_1$ ,  $\theta_2$  and  $\theta_3$ . Then it is easy to see that  $Z_1$  is found at the event corresponding to  $\theta'$ . For example, if  $\theta' = \theta_1$ , when  $u$  and  $v$  are aligned horizontally, there exists exactly one point  $t$  on  $e_2$  that realizes the *h-alignment* of  $e_1$  and  $e_2$ , and  $\bar{\eta}(t)$  meets  $u$  and  $e_1$ . Thus there exists at most one edge that is *t-aligned* with  $e_1$  and  $e_2$ , which should be  $e_l$  by *t-alignment* of  $(e_1, e_l, e_2)$ . Moreover,  $\bar{\delta}(\bar{\eta}(u)) = \bar{\delta}(\bar{\eta}(t))$  is on  $e_l$ , which allows us to detect  $(e_1, e_l, e_2)$  at  $\theta'$ . Similarly, there are eight events corresponding to  $Z_2$ , four events are of case (1) and others are of case (2). Then  $Z_2$  is found at the smallest orientation among the orientations that the eight events occur since all incident pairs and triplets of edges in  $Z_2$  are *h-*, *v-* or



t-aligned until the smallest orientation. Thus we find all DSs of type F. Since we compute the maximal configuration and breaking configuration which contain a cc on a vertex of  $P$  whenever we find a DS, all maximal configurations and breaking configurations of type F which contains a cc on a vertex of  $P$  are computed.  $\square$

There are  $O(n^2)$  events corresponding to case (1) and  $O(n^3)$  events corresponding to case (2). We can compute them in  $O(n^3)$  time in total. For each event, we find  $O(1)$  DSs in  $O(\log n)$  time and compute  $O(1)$  maximal and breaking configurations of each DS in  $O(1)$  time, and check their feasibility in  $O(\log n)$  time. And the only data structure we use for type F is a ray-shooting data structure of  $O(n)$  space. By lemmas 22 and 24, we can conclude with the following lemma.

**Lemma 25** *We can compute a largest rectangle among all LMRs of type F in  $O(n^3 \log n)$  time using  $O(n)$  space.*

## 8 Computing a largest rectangle in a simple polygon with holes

Our algorithm can compute a largest rectangle in a simple polygon  $P$  with  $h$  holes and  $n$  vertices. We use the same classification of largest rectangles and find the LMRs of the six types. We construct a ray-shooting data structure, such as the one by Chen and Wang [7] in  $O(n + h^2 \text{polylog } h)$  time using  $O(n + h^2)$  space, which supports a ray-shooting query in  $O(\log n)$  time. We also construct the visibility region from each vertex of  $P$ , which can be done in  $O(n^2 \log n)$  time using  $O(n^2)$  space by using the algorithm in [7]. Each visibility region is simple and has  $O(n)$  complexity. The staircase of a vertex of  $P$  can be constructed in  $O(n \log n)$  time using plane sweep with ray-shooting queries. Each staircase of a vertex  $u$  of  $P$  has  $O(n)$  space. There are  $O(n^2)$  events to the staircase of  $u$  since it is equivalent to the staircase constructed in  $V(u)$ , a simple polygon with  $O(n)$  vertices.

We say a rectangle is *empty* if there is no hole contained in it. Since  $P$  has holes, there can be a hole contained in a rectangle  $R$  even though every side of  $R$  is contained in  $P$ . Thus, we check the emptiness of rectangles, together with the test for their sides being contained in  $P$ . The emptiness of a rectangle can be checked by constructing the triangular range searching data structure proposed by Goswami et al. [10]. Given a set of  $n$  points in the plane, the triangular range searching data structure can be constructed in  $O(n^2)$  time and space such that given a query triangle, the number of points lying in the triangle can be answered in  $O(\log n)$  time. We consider the  $n$  vertices of  $P$  as the input points to the data structure and consider a rectangle as a query with two triangles obtained from subdividing the rectangle by a diagonal. Then we can check the emptiness of a rectangle in  $O(\log n)$  time. Since the remaining part of our algorithm works as it is, we have Theorem 1.

## 9 Computing a largest rectangle in a convex polygon

When  $P$  is convex, there is no reflex vertex and therefore it suffices to consider only the LMRs of types A and F. For type A, we take two vertices  $v$  and  $u$  and check if the square with  $vu$  as a diagonal is contained in  $P$  using ray-shooting queries. Among such squares, the one with largest area is the largest LMR of type A in  $P$ , by Lemma 7. Thus, using the method in Lemma 8, we can compute a largest LMR of type A in  $O(n^2 \log n)$  time using  $O(n)$  space.

For type F, we find the events considered in Section 7 and all DSs corresponding to the events in case (1) that a vertex  $u$  is aligned to another vertex in  $O(n)$  time by maintaining rays  $\lambda(u)$ ,  $\delta(\bar{\lambda}(u))$ ,  $\delta(u)$  and  $\lambda(\bar{\delta}(u))$  during the rotation. Since  $P$  is convex, the foot of each ray emanating from  $u$  changes *continuously* along the boundary of  $P$ . Similarly, we find all DSs corresponding to the events in case (2) in Section 7 that an edge triplet becomes t-misaligned. It is caused by  $\bar{\delta}(\bar{\eta}(u))$  meeting  $p$  for a vertex pair  $(u, p)$  and its corresponding DSs can be computed in  $O(n)$  time by maintaining  $\eta(u)$ ,  $\delta(u)$ ,  $\xi(p)$  and  $\lambda(p)$  during the rotation, where  $\xi(p)$  is the vertically upward ray from  $p$ . Thus, we can find all events and their corresponding DSs in  $O(n^2)$  time for case (1) and in  $O(n^3)$  time for case (2). Since every LMR is contained in  $P$ , we can find the maximal configuration of each DS in  $O(1)$  time. We conclude with Theorem 2.

## 10 Discussion

We study the problem of finding a maximum-area rectangle with no restriction on its orientation that is contained in a simple polygon  $P$  with  $n$  vertices in the plane and present  $O(n^3 \log n)$ -time algorithm. One may wonder if the algorithm can be improved. It is shown that there can be  $\Omega(n^3)$  combinatorially distinct rectangles even when  $P$  is convex [6]. So any algorithm that iterates over all combinatorially distinct rectangles contained in  $P$  needs at least  $\Omega(n^3)$  time, and therefore there seems hardly any room to improve, except improving it by  $\log n$  factor.

## References

- [1] Alok Aggarwal and Joel Martin Wein. *Computational Geometry Lecture Notes for MIT*. 18.409. 1988.
- [2] Helmut Alt, David Hsu, and Jack Snoeyink. Computing the largest inscribed isothetic rectangle. In *Proceedings of 7th Canadian Conference on Computational Geometry (CCCG 1995)*, pages 67–72. University of British Columbia, 1995.
- [3] Nina Amenta. Bounded boxes, Hausdorff distance, and a new proof of an interesting Helly-type theorem. In *Proceedings of 10th Annual Symposium on Computational Geometry (SoCG 1994)*, pages 340–347, 1994.
- [4] Sang Won Bae, Chunseok Lee, Hee-Kap Ahn, Sunghee Choi, and Kyung-Yong Chwa. Computing minimum-area rectilinear convex hull and L-shape. *Computational Geometry*, 42(9):903–912, 2009.
- [5] Ralph P. Boland and Jorge Urrutia. Finding the largest axis-aligned rectangle in a polygon in  $O(n \log n)$  time. In *Proceedings of 13th Canadian Conference on Computational Geometry (CCCG 2001)*, pages 41–44, 2001.
- [6] Sergio Cabello, Otfried Cheong, Christian Knauer, and Lena Schlipf. Finding largest rectangles in convex polygons. *Computational Geometry*, 51:67–74, 2016.
- [7] Danny Z. Chen and Haitao Wang. Visibility and ray shooting queries in polygonal domains. *Computational Geometry*, 48(2):31 – 41, 2015.
- [8] Karen Daniels, Victor Milenkovic, and Dan Roth. Finding the largest area axis-parallel rectangle in a polygon. *Computational Geometry*, 7(1):125–148, 1997.
- [9] Paul Fischer and Klaus-Uwe Höffgen. Computing a maximum axis-aligned rectangle in a convex polygon. *Information Processing Letters*, 51(4):189–193, 1994.
- [10] Partha P. Goswami, Sandip Das, and Subhas C. Nandy. Triangular range counting query in 2d and its application in finding  $k$  nearest neighbors of a line segment. *Computational Geometry*, 29(3):163 – 175, 2004.
- [11] Olaf Hall-Holt, Matthew J. Katz, Piyush Kumar, Joseph S. B. Mitchell, and Arik Sityon. Finding large sticks and potatoes in polygons. In *Proceedings of 17th Annual ACM-SIAM Symposium on Discrete Algorithm (SODA 2016)*, pages 474–483, 2006.
- [12] John Hersberger and Subhash Suri. A pedestrian approach to ray shooting: Shoot a ray, take a walk. *Journal of Algorithms*, 18(3):403–431, 1995.
- [13] Christian Knauer, Lena Schlipf, Jens M. Schmidt, and Hans Raj Tiwary. Largest inscribed rectangles in convex polygons. *Journal of Discrete Algorithms*, 13:78–85, 2012.
- [14] Michael McKenna, Joseph O’Rourke, and Subhash Suri. Finding the largest rectangle in an orthogonal polygon. In *Proceedings of 23rd Allerton Conference on Communication, Control and Computing*, pages 486–495, 1985.
- [15] Derick Wood and Chee K. Yap. The orthogonal convex skull problem. *Discrete & Computational Geometry*, 3(4):349–365, 1988.

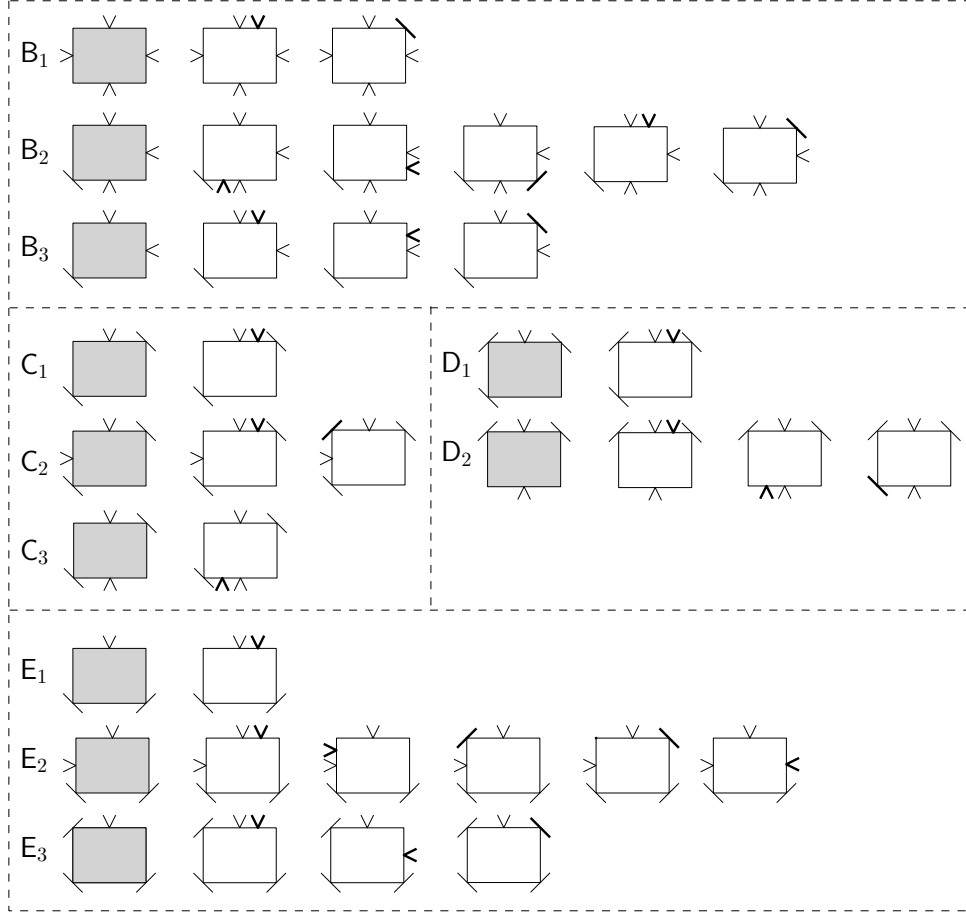


Figure 10: Canonical (sub)types (gray rectangles) and their breaking configurations without duplication. The breaking configurations of subtypes  $F_1$  and  $F_2$  appear as breaking configurations of other types: By adding a sc to a DS  $Z$  of type  $F_1$ ,  $Z$  becomes a BC of type either  $D_1$  or  $E_3$ . By adding a cc to a DS  $Z$  of type  $F_1$ ,  $Z$  becomes a BC of type  $F_2$ . By adding a sc to a DS  $Z$  of type  $F_2$ ,  $Z$  becomes a BC (of the last type) of type  $E_3$ .